Deanship of Graduate Studies

Al-Quds University

Single Molecule Based Nanoelectronic Devices

Imad Abdulla Ahmad Ibrahim

M.Sc. Thesis

Jerusalem - Palestine

2007

Single Molecule Based Nanoelectronic Devices

Prepared by:
Imad Abdulla Ahmad Ibrahim

B.Sc. Electronic Engineering. Al-Quds University-Palestine

Supervisor: Dr. Mukhles Sowwan

A thesis Submitted in Partial fulfillment of requirements for the degree of Master of Computer and Electronic Engineering Program at Faculty of Engineering, Al- Quds University.

2007

Al-Quds University
Deanship of Graduate Studies
Computer and Electronic Engineering Program

Thesis Approval

Single Molecule Based Nanoelectronic Devices

Prepared by: Imad Abdulla Ahmad Ibrahim
Registration No.: 20320122

Supervisor: Dr. Mukhles Sowwan

Master thesis submitted and accepted, Date: 12 / 6 / 2007
The names and signatures of the examining committee members are as follows:

1-Head of Committee:	Dr. Mukhles Sowwan	Signature
2-Internal Examiner:	Dr. Husein Jaddu	Signature
3-External Examiner:	Dr. Edward Sader	Signature

Jerusalem - Palestine

2007

Dedication

To my parents, my wife and my family

Imad A A Ibrahim

Declaration:

I certify that this thesis submitted for the degree of Master is the result of my own research, except where otherwise acknowledged, and that this thesis (or any part of the same) has not been submitted for a higher degree to any other university or institution.

Signed: 

Imad Abdulla Ahmad Ibrahim

Date: 12 / 6 / 2007

Acknowledgements

At the end of my thesis I would like to thank all those people who made this thesis possible and an enjoyable experience for me.

First of all I wish to express my sincere gratitude to my supervisor Dr. Mukhles Sowwan who guided and advise me throughout this work with patience and help. Also I express my deepest gratitude to Dr. Jamal Ghaboun, , Mr. Ishaq Issa, and my colleges in Nanotechnology Research Laboratory for their help.

Finally, I would to like my family for their help and encouragement, especially my wife Rasha and My brother Dr. Murad.

Abstract

The implementation of electronic devices and increasing their efficiency has been central to science and technology in many ways in the second half of the last century. Molecular nanoelectronics have started to gain a growing attention over the last decade. A Nanoelectronic concept based on protein-nanoparticle hybrids is implemented throughout this work. Here we developed a building block for Lego like fabrication of nanoelectronic devices, where gold Nanoparticles (GNP) are embedded in the central cavity of a ring shaped like protein that is named stable protein 1 (SP1). The gold-Nanoparticles are with diameter of 1.8 nm, and they are the active components of the nanoelectronic device. SP1 is a ring shaped like protein with outer diameter 10nm, inner diameter 4 nm, and height 2.5 nm. This protein is a stable, resistant to high temperatures, stress-responsive and homo-oligomeric protein isolated from popular trees, genetically engineered to have suitable dimensions and characteristics that enable fixing gold nanoparticles into its central cavity. Single SP1-GNP unit is built and characterized, in addition ssDNA molecules with suitable sequences and lengths are assembled with SP1-GNP complex. As a results, long one dimensional nanowires, and a two dimensional arrays that can serve as memory device are produced.

A conductive Atomic Force Microscope (AFM) tip is used to investigate, characterize and electrically polarize the SP1 molecules and SP1-GNP nanostructures in several modes. Tapping mode atomic force microscopy was used for morphological characterization of the protein and protein gold nanoparticle hybrids, the cross sectional height profiles showed that the height of bare SP1 deposited on solid substrate is 2.5 nm; while the height of the SP1-gold nanoparticle is 3.2 nm. Polarizability of the SP1-GNP block was studied using Electrostatic Force Microscopy in which both positive and negative voltages are applied on the tip of AFM and measure the response of SP1-GNP unit toward this voltage; the results showed that the bare SP1 is silent while the SP1 gold hybrid is polarizabe.

الملخص

إن تصنيع القطع الالكترونية ذات الخصائص المطورة و الفاعلية العالية والتكلفة القليلة أصبح من الاهتمامات الرئيسية للأبحاث العلمية والتكنولوجية خلال النصف الثاني من القرن الماضي، كما أن الالكترونيات المتناهية في الصغر المصنعة من الجزيئات الحيوية جلبت المزيد من الاهتمام والتركيز خلال العقد الأخير، لما لها من خصائص تمكن الباحثين من إنتاج قطع ذات فاعلية عالية وتكلفة قليلة، في هذا البحث قمنا بدراسة مبدأ جديد للالكترونيات يقوم على إنتاج قطع الكترونية من خلال الدمج بين نوع من البروتينات النباتية وجزيئات الذهب، لقد حاولنا في هذا البحث إنتاج وحدة أساسية للقطع الالكترونية من خلال زرع جزيئات الذهب (ذات القطر 1.8 نانومتر) في مركز احد أنواع البروتينات النباتية التي تشبه الحلقة (القطر الخارجي 10 نانومتر، القطر الداخلي 4 نانومتر و الارتفاع 2.5 نانومتر) مستفيدين من أن البروتين (SP1) يتم استخراجه من احد أنواع النباتات الصحراوية بتكلفة قليلة ويمتاز بالثبات مع الوقت و تحمل التغيرات الحرارية والضغط العالي، بحيث تم تعديل جزيئات البروتين جينيا لتصبح ذات أبعاد و خصائص تساعد في تثبيت كريات الذهب داخل جزيئات البروتين. من خلال هذا البحث تم إنتاج وحدات من بروتين (SP1) وجزيئات الذهب، وبعد إضافة جزيئات الحمض الريبوزي المصنعة (DNA) ذات الترتيب والطول المناسب إلى محلول وحدات البروتين (SP1) وجزيئات الذهب تم إنتاج أسلاك صغيرة جدا من وحدات البروتين (SP1) وجزيئات الذهب مرتبطة معا بواسطة الحمض النووي الرايبوزي، كما تم إنتاج مصفوفة من وحدات البروتين (SP1) وجزيئات الذهب.

تم استخدام مجهر القوى الذرية في فحص و تشخيص وحدات البروتين (SP1) وجزيئات الذهب من حيث الارتفاع والخصائص الكهربائية، من خلال النتائج تبين أن ارتفاع جزيء البروتين (SP1) هو 2.5 نانومتر، بينما ارتفاع وحدة البروتين (SP1) وجزيئات الذهب هو 3.2 نانومتر. أما الخصائص الكهربائية فقد تم دراستها من خلال التأثير على جزيئات البروتين (SP1) و وحدات البروتين (SP1) وجزيئات الذهب بفرق جهد كهربائي موجب وسالب وتسجيل تأثير فرق الجهد على قابلية التأين والشحن للجزيئات المختلفة، من خلال دراسة النتائج تبين أن جزيئات البروتين (SP1) غير قابلة للتأين، بينما وحدات البروتين (SP1) وجزيئات الذهب قابلة للتأين.

Table of Contents

1. Introduction and Motivation …… 1

2. Methods and Materials …… 6

2.1 Atomic Force Microscopy…….. 7

2.1.1 Principle…….. 7

2.1.2 Probe Sample Interactions…….. 9

2.1.3 AFM probes (Force Sensors)…….. 11

2.1.4 Imaging Modes…….. 13

2.1.5 Image Interpretation …….. 15

2.2 Electrostatic Force Microscopy via AFM……. 16

2.2.1 Principle…….. 16

2.2.2 Interpretation of the EFM image…….. 18

2.2.3 EFM Modes…….. 19

2.3 Force Distance Curves (FZ) via AFM…… 20

2.4 Materials …… 22

3. Architecture of SP1 protein-Gold nanoparticle based Nanoelectronic devices ……. 26

3.1 The Basic Building Block…….. 27

3.2 Possible nano-Electronic Devices Architecture …… 28

3.2.1 Molecular wire…….. 28

3.2.2 Ultra High density Memory…….. 30

4. Results and Discussion…… 31

4.1 Characterization of SP1 …… 32

4.1.1 Morphological characterization of SP1 Molecules ……. 32

4.1.2 EFM Images…….. 33

4.2 Characterization of SP1-GNP Hybrids ……. 34

4.2.1 Morphological characterization of SP1-GNP Hybrids… 35

4.2.2 EFM Images…….. 37

4.3 Ligo like fabrication of nano-electronic devices……. 38

4.3.1 SP1-GNP Nano-wires 38
4.3.2 SP1-GNP Array 41

5. Conclusion and Future Work 43
5.1 Conclusion..... 44
5.2 Future Work..... 44

References 45

List of Figures

Figure Number	Figure Name	Page
Figure 2.1	*Schematic illustration of the meaning of "spring constant" as applied to cantilevers. Visualizing the cantilever as a coil spring, its spring constant k directly affects the downward force exerted on the sample*	8
Figure 2.2	*Schematic of an Atomic Force Microscope*	8
Figure 2.3	*Beam-deflection set-up for the simultaneous detection of lateral and vertical force components*	9
Figure 2.4	*Scheme of an AFM probe: a sharp tip mounted on a cantilever*	10
Figure 2.5	*Typical illustration of forces involved in AFM*	11
Figure 2.6	*SEM images of different tips*	12
Figure 3.7	*(a)SEM image of NSG10 cantilever holding a tip connected to the holder chip, (b) SEM image of NSG10 tip with height (10 -15 µm), cone angle ≤22^0 and curvature radius of 10 nm,(c) schematic of NSG10 chip and cantilever, (d) NSG10 tip schematic*	13
Figure 2.8	*Tip convolution effect on the imaged objects*	15
Figure 2.9	*EFM schematic setup*	16
Figure 2.10	*Schematic of the EFM "plane mode" operation*	19
Figure 2.11	*(a) SEM image of NSG03/Pt tip with height (10 -15 µm), cone angle ≤22^0 and curvature radius of 35 nm,(c) schematic of NSG10 chip and cantilever, (d) NSG10 tip schematic*	20
Figure 2.12	*F-Z Technique setup*	21
Figure 2.13	*(a) 3-D structure of an SP1 dodecamer elucidation from X-ray crystallography. (b) Electron microscopy of SP1 stained with uranyl-acetate. Average of 313 top-view aligned particles (scale bar 10 nm). (c) SP1-protein array prepared by the water/phospholipid coating method and observed with TEM*	23
Figure 2.14	*Crystal structure of an SP1 dodecamer showing the N-*	23

	termini of SP1 pointing from the central cavity to the opposite planes of the ring, in a way that 6 N-termini point to one side (perpendicular into the screen) and 6 N-termini point to the opposite side.(perpendicular out of the screen).	
Figure 3.1	*(a) Crystal structure of an SP1 dodecamer showing the N-termini of SP1 (b,c) A computer simulation of the hybrid in a top and side views. (d-f) HAADF-STEM images of two top views (d,e) and side view (f) of the SP1-GNP hybrid (scale bar: 10 nm)*	28
Figure 3.2	*(MW) DNA ladder;phi X 174DNA/Hinf I, (a,b) nonannealed ssDNA, (c,d) annealed dsDNA*	29
Figure 3.3	*(a) 80bp ssDNA ended with thiol (b) thiolated 22 bp ssDNA, (c) SP1-GNP hybrid, (d) SP1-GNP hybrids connected via long dsDNA (e) SP1-GNP hybrids connected via 22bp dsDNA*	30
Figure 3.4	*(a) Schematic of SP1-GNP hybrid (b) Schematic representation of the proposed memory cell*	30
Figure 4.1	*(a) AFM Topography images of SP1protein without gold-nanoparticle acquired in tapping mode, (insert) cross section showing the height of SP1 molecules (c) histogram shows SP1 molecules heights distribution*	32
Figure 4.2	*FZ-curves for SP1 complex with (a) zero bias voltage (Sample-tip distance = 50.7nm), (b) +5 bias voltage (Sample-tip distance = 51.2 nm), (c) -5 bias voltage*	33
Figure 4.3	*(a) AFM topography image of SP1 molecules without GNP, "insert" cross section shows the height of SP1 molecule indicated on topography image, (b,c,d) Phase images for the area recorded in (a) with various bias voltages applied to the tip +5V, 0V and -5V respectively, "insert" cross section shows the phase shift in volts*	34
Figure 4.4	*(a) AFM topography image of SP1-GNP hybrid (insert) cross section of height profile of two SP1-GNP units, (b) histogram shows SP1 molecules heights distribution)*	35
Figure 4.5	*(a) Topography image of single SP1-GNP hybrid, (b) A computer simulation of theSP1-GNP hybrid in a top view, (c) HAADF-STEM images of the SP1-GNP hybrid in a top view, (d) Filtered Image of (a) with Laplace filter, (d) 3D image of the filtered image shown in (d), (f) Contour image for the block shown in (a)*	36
Figure 4.6	*FZ-curves for SP1-GNP complex with (a) zero bias voltage*	37

	(Sample-tip distance = 63 nm), (b) +5 bias voltage (Sample-tip distance = 62.9 nm), (c) -5 bias voltage	
Figure 4.7	*(a) AFM topography image of SP1-GNP unit (insert) cross section shows the height of SP1-GNP unit (b) Phase image of the SP1-GNP unit in (a) with bias voltage +5V (insert) cross section shows the EFM signal on the SP1-GNP indicated in (a), red curve is due to +5V bias, blue curve is due to 0V and green curve is due to -5V bias*	37
Figure 4.8	*(a) AFM topography image of SP1-GNP units (b,c,d) Phase images of the SP1-GNP units in (a) with bias voltage +5V, 0V and -5V V, respectively (e) cross section shows the height of SP1-GNP unit as indicated in (a) (height 3.2 nm), (f) cross section shows EFM signal on the SP1-GNP indicated in (a), red curve is due to +5V bias, blue curve is due to 0V and green curve is due to -5V bias*	38
Figure 4.9	*(a) AFM imaging of SP1 with GNP once shown with a dsDNA-ended with thiol connection (white arrow) of 22bp of length and once without (black arrow) (b,c,d insert) Cross sections of height profiles extracted from AFM scanning showing the different heights of the two pairs of SP1-GNP (e) Contour image shows the position of GNP in the central cavity of SP1*	39
Figure 4.10	*Different examples of SP1-GNP nanowires*	40
Figure 4.11	*(a) AFM topography imaging of SP1-GNP-DNA forming a wire like behavior (insert) Height diagram corresponding to the cross section shown (b) Phase shift image for an EFM process applied on the same SP1-GNP-dsDNA combination shown in (a)(c,d,e) EFM profiles corresponding to the cross section shown in (b) for +5V, 0V and -5V, respectively)*	41
Figure 4.12	*A TEM image of a self-assembled 2D crystalline array of recombinant SP1-GNP molecules formed under a charged lipid layer*	41
Figure 4.13	*(a,d) AFM topography image of SP1-GNP hybrid acquired with taping mode (b,c) cross section shows heights for SP1-GNP units from images (a), height is in the range (3 nm – 3.4nm)*	42

Definitions

AFM	Atomic Force Microscopy
bp	base pair
CM	Contact Mode
DNA	Deoxyribonucleic Acid
dsDNA	Double Strand Deoxyribonucleic Acid
EFM	Electrostatic Force Microscopy
FZ Curves	Force Distance Curves
GNP	Gold nanoparticles
HAADF-STEM	high-angle annular dark-field scanning transmission electron microscopy
NCM	*Non Contact Mode*
SFM	Scanning Force Microscopy
SP1	Stable Protein 1
STM	Scanning Tunneling Microscope
ssDNA	Single Strand Deoxyribonucleic Acid
2D Array	Two Dimensional Array
3D Mode	Three Dimension Mode

Chapter ONE

Introduction and Motivation

Chapter ONE

Introduction and Motivation

Need is the mother of invention. The need of new electronic devices with improved characteristics leads the scientists and researchers, in the field of electronic devices fabrication, to enter a race interests in fabricating new devices. These new devices must have characteristics that overlap the limitations and disadvantages of the existed devices fabricated with the common methods. Those researchers try to develop techniques that create new devices with smaller size, cost-effective, less energy consumption and efficiently operated.

As semiconductors components become very small, their dimensions goes from one metric scale “micro” to a smaller one “nano”. A new term is created and spread between the semiconductor manufacturer and researcher, which is nano-technology. The first time the term “nanotechnology” was used, was in 1976 by Norio Taniguchi, a Tokyo Science University professor, and made popular by K. Eric Drexler in his book "Engines of Creation", where his seminal work on the topic published in 1986 (NOVA Workforce Board 2003). The prefix nano representing 10^{-9} (0.000000001), and the term nanotechnology - according to NASA Ames Research Center- is defined as the creation of functional materials, devices and systems through control of matter in the range of one-tenth to one-hundred nanometer (0.1-100 nm) and the exploitation of novel phenomena and properties in this scale (NOVA Workforce Board 2003). This technology enables a scientific and technical revolution based upon the ability to systematically organize and manipulate matter at the atomic scale.

It’s believed that the nanotechnology is the next great technology wave, the nexus of scientific innovation and industrial revolutions indirectly affect the fabric of society. This is because there are various unique properties of matter that are expressed in the nanoscale and are quite foreign to our bulk statistical senses (Jurveston 2004).

Nanotechnology has the potential to transform materials and manufacturing, and research is driven by the need to improve functionality of materials, and it has the potential to have big impact. Potential applications include the expansion of increasingly greater amount of data storage on an increasingly smaller scale, and the synthesis of all components related to computer technology, including wiring and connection (The White House-Office of the Press Secretary 2000).

One of the most powerful methods in nanoelectronic devices fabrication technology is e-beam lithography; which is the practice of using a beam of electrons to generate patterns on a surface in the 100 nm size range (Brain 2001). This form of lithography has found wide usage in research, but has not yet become a standard technique in industry, this is due to many reasons; the most important one is the huge cost of starting up such technique, other reason is the physical limitation of the raw materials used in this technique which is silicon (ITRS 2001), it is hard to imagine and achieve smaller devices with atomic resolution using this technique (Jurveston 2004).

An alternative solution that overlapping the drawbacks of the current technology is biology based nanoelectronics, i.e Molecular electronics, because of its three important features (Fabio 2004); recognition, structuring and conductivity; this means that biology molecules have the ability to bind to one another, recognize each other or external electrode, assemble into larger structures, transport efficiently carriers from one point to another. In addition, individual molecules are hundreds of times smaller than the smallest features conceivably attainable by current semiconductor technology; because it is the area taken up by each electronic element that matters, electronic devices constructed from molecules will be hundreds of times smaller than their semiconductor-based counterparts. Moreover, individual molecules such as Deoxyribonucleic acid (DNA) and proteins are easily made exactly the same by the billions and trillions, which is related to structuring feature of biological molecules. The dramatic reduction in size and the sheer enormity of numbers in manufacture are the principle benefits offered by the field of molecular electronics.

Self-assembly and applications of DNA in nanoelectronics is investigated through out many experiments. Polyakov and his partners report that DNA has the ability to self-assembly on the mica surfaces and the Au(111), they use the Atomic Force Microscope in their study (Polyakov 2003).

Natural functional characteristics of proteins that result a natural electron transfer activity in addition to the self-assembling nanostructures and the strong bonds between the protein fibrils (Erika 2003); makes proteins to be believed as a novel and a valuable building blocks for nanotechnology applications. Nature has selected, evolved and produced proteins that can interact and self-organize to create sophisticated nano-machines and nanostructures (Sarikaya 2003). Due to these important features proteins are used in the realization of molecular switches and in the implementation of a prototype of protein transistor operating in air and in the solid state (Ross 2003).

Tunneling properties of a number of metalloproteins including blue copper protein azurin, where the copper atom is situated approximately 7Å from the protein surface, asymmetrically embedded in a hydrophobic core (Lontie 1984). Then the ability of binding azurin molecule to gold substrate by using the tip of atomic force microscope is studied (Davis et al, 2004). In addition, effect on mica after incubation in azurin solution is illustrated, and the self-assembly of azurin on mica is clearly visible (Andrea 2003).

Erika and partners produced conducting wires from engineered fibrils bond tightly with gold nanoparticles (Erika 2003), these wires can be used in small-scale circuitry, biosensors in addition to other applications.

Nanoscale ordered arrays of metal and semiconductor quantum dots are fabricated by binding preformed nanoparticles onto crystalline protein templates made from genetically engineered hollow double-ring structures called chaperonins, which are subcellular structures composed of 14, 16, or 18 subunits called heat shock proteins (HSP60). (Andrew 2002).

In this work, nanoelectronic concepts based on protein-nanoparticle hybrids was implemented. SP1 (Stable Protein 1) was used. This protein is a stable one that is isolated from popular trees, forming a ring shaped with outer diameter of 10 nm and inner diameter of 4 nm (Wang 2003) to make a building block, or in other words, a unit cell consists of gold nanoparticles that serves as quantum dot, embedded in the central cavity of an SP1 protein. The gold nanoparticle-SP1 complex is assembled in nanowires where thiolated DNA molecules with different lengths and sequences are assembled with SP1-GNP complexes, or monolayer arrays attached to a suitable substrate. A conductive AFM tip is used to investigate, characterize and electrically polarize the SP1- gold nanostructures.

My work in this research passes the following main phases, i. Characterization of bare SP1 protein and the SP1-gold nanoparticle complexes using tapping mode atomic force microscopy (AFM) ii. Electrical Characterization and polarization of the SP1-gold nanoparticles complexes using AFM.

This thesis includes five chapters; Chapter one is general introduction and Motivation. Chapter two includes methods and materials used through out this work, The SP1 protein, gold nanoparticles (GNP) and substrate materials. Also an introduction to the atomic force microscopy; the main instrument and technique used in this study available in our laboratory; and its different modes of operation are outlined. How to build an electronic device such as a nanowire or memory devices from SP1-gold nanoparticle complex is explained in chapter three.

Measurements collected throughout the research phases are reported and discussed with details in chapter four. Finally, conclusions, suggested future work are registered in chapter five.

Chapter TWO

Methods and Materials

Chapter TWO

Methods and Materials

2.1 Atomic Force Microscopy

In 1980/81 G. Binnig, H. Rohrer, and coworkers from IBM Zürich Research Laboratories invented a new type of microscope (Binnig 1982) which they called the Scanning Tunneling Microscope (STM) (Binng 1985).

When looking back it is evident that the outstanding success of STM is not only due to the ultrahigh resolution which can be achieved by this technique. Equally important, if not more, is that STM stimulated the development of a whole family of Scanning Probe Methods (SPM) which is all based on instrumental principles very similar to that of the STM (Hartmann 1997). These scanning probe methods must achieve two essential aspects: scanning and operating the scanned probe in near-field (Hartmann 1997). Binnig and his partners continue their work to develop new instrument which they named Atomic force microscope (AFM) which enables us to have a look on surfaces on a molecular level; AFM became later the most popular scanning probe technique because it overcomes the limitation of STM in imaging thin samples on electrically conductive materials. In addition to the high resolution, atomic force microscope offers the possibility to characterize mechanical properties, such as hardness, and surface forces, such as adhesion force of the samples in the nanometer scale.

2.1.1 Principle

Like all other scanning probe microscopes, AFM utilizes a sharp probe moving over the surface of a sample in a raster scan. The probe is a tip at the end of a cantilever which bends in response to the force between the tip and the sample. Figure 2.1 shows the basic principle of AFM which is visualized as a cantilever with a spring constant weaker than the equivalent spring constant between atoms (Binng 1986).

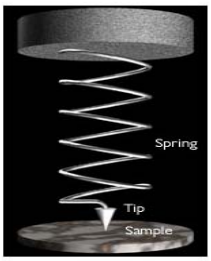

Figure 2.1: *Schematic illustration of the meaning of "spring constant" as applied to cantilevers. Visualizing the cantilever as a coil spring, its spring constant k directly affects the downward force exerted on the sample.*

Together with a mass m of the atoms in the order of 10^{-25} kg, an interatomic spring constants k of about 10 N/m is received. By sensing Ångstrom-size displacements of such a soft cantilever spring, one can image atomic-scale topography. Furthermore, the applied force will not be large enough to push the atoms out of their atomic sites.

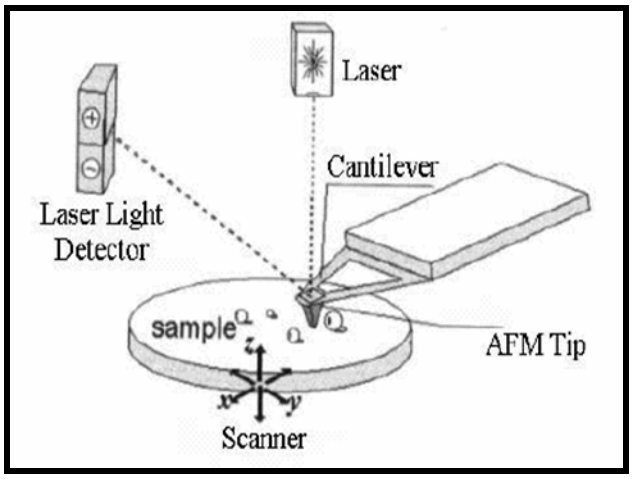

Figure 2.2: *Schematic of an Atomic Force Microscope (www.keele.ac.uk/depts/ch/groups/csg/pat/pathome.htm)*

The tip (that part which directly interacts with the sample) is mounted on the cantilever as shown in Figure 2.2 which is a schematic of AFM. Forces between tip and sample deflect the cantilever. The cantilever's deflection is detected and converted into an electronic signal that is utilized to reconstruct an image of the surface. One of the most utilized

methods to detect the cantilever deflections is the optical method: It consists in focusing a laser beam on the back of the cantilever and measuring the displacements of the reflected beam on a multiple segment photodiode. The corresponding signals are acquired and processed by feedback electronics. The feedback system is used to control the cantilever deflection and to direct consequently the piezoelectric scanner movements. Usually, the sample is mounted onto a piezoelectric translator that moves the sample in the x, y and z directions underneath the tip. When the tip translates laterally (horizontally) relative to the sample surface, one measures the sample topography.

The cantilever deflection is measured by detecting the related displacement of a laser beam reflected off the back of the cantilever. Spatial variations of the reflected laser beam are detected by a position-sensitive photo-detector as the one appears in Figure 2.3, segmented into four quadrants. When the light beam moves between the upper and lower pairs of segments the deflection of the cantilever can be deduced from a proper treatment of all individual photocurrents.

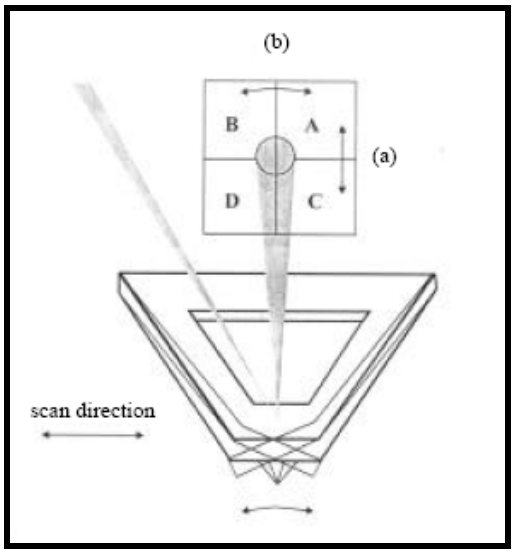

Figure 2.3: *Beam-deflection set-up for the simultaneous detection of lateral and vertical force components.*

2.1.2 Probe Sample Interactions

The forces that contribute to the force exerted on the tip can be divided in three groups: (i) surface forces, (ii) forces due to the sample deformation and (iii) the elastic force of the cantilever. All three forces can be of either sign. Figure 2.4 shows a scheme of the three types of the forces that affect the tip-sample explaining the direction of the effect for each.

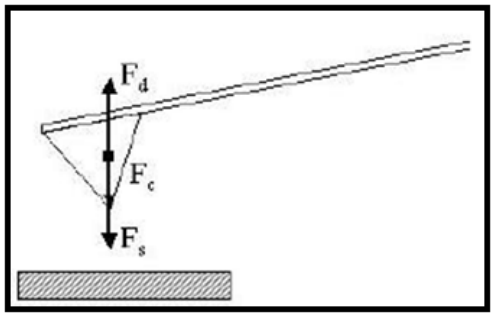

Figure 2.4: *Scheme of an AFM probe: a sharp tip mounted on a cantilever.*

(i) Surface forces (Fs). An elementary constituent of the interaction between a flat, rigid substrate and a sharp, rigid tip in vacuum is the pair potential between atoms at the tip and the sample. The origin of the intermolecular forces is essentially electromagnetic. At large distances (~1-30 nm) the forces are attractive and are described by a van der Waals pair potential.

(ii) Forces due to the deformation of samples (Fd). So far the tip of the AFM and the sample has been assumed to be rigid. While this is often a good approximation for the tip, samples are often significantly deformed elastically by the tip. The simplest approach to describe elastic deformation of the sample is the Hertz theory (Israelachvili 1992)

(iii)Elastic force of the cantilever (Fc). The interaction forces between sample and tip are balanced by the elastic force due to the cantilever bending. Summarizing, the deflection of the cantilever results from a combination of deformation and surface force.

The above mentioned forces are for any given experiment since it represents the general behavior of two solids brought into sufficiently close proximity. However, a couple of additional interactions can result if suitable environmental conditions are chosen or if external manipulations are undertaken in a suitable way. If an electrical potential is applied between probe and sample, Coulomb interactions provide an additional long-range attractive contribution. Charges of equal sign on probe and sample would in contrast lead to repulsive forces. If probe and sample consist of ferromagnetic materials the resulting long-range magnetostatic interactions can either be repulsive or attractive. Figure 2.5 summarize the tip-sample forces versus the distance in between.

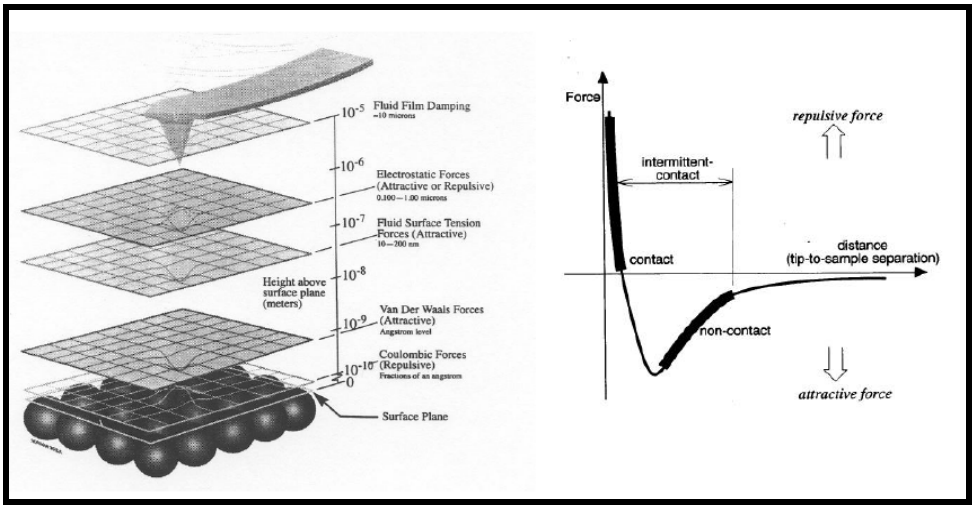

Figure 2.5: *Typical illustration of forces involved in AFM (www.pacificnano.com/afm-modes_single.html)*

2.1.3 AFM probes (Force Sensors)

In order to detect local forces or closely related physical quantities the sharp probe scanning the sample surface at some distance has to be linked to some sort of force sensor. A convenient way to precisely measure forces is to convert them into deflections of a spring according to Hooke's law.

In SFM the force-sensing spring consists of a miniaturized cantilever beam clamped at one end and equipped with the probing tip at the other end. While at the beginning tiny pieces of thin metal foils were equipped with glued diamond tips (Binnig 1986), electrochemically etched metal wires were subsequently found to be easier to handle (Lemke et al, 1990). The increasing demand for cantilevers with integrated sharp tips, tailored reproducibly, and for the availability of a large number of them soon led to the development of microfabrication techniques based on the machining of Si-related materials (Albrecht 990). Today a variety of cantilevers with different geometries (mainly bar- and V-shaped) and with pyramidal as well as conical tips is commercially available.

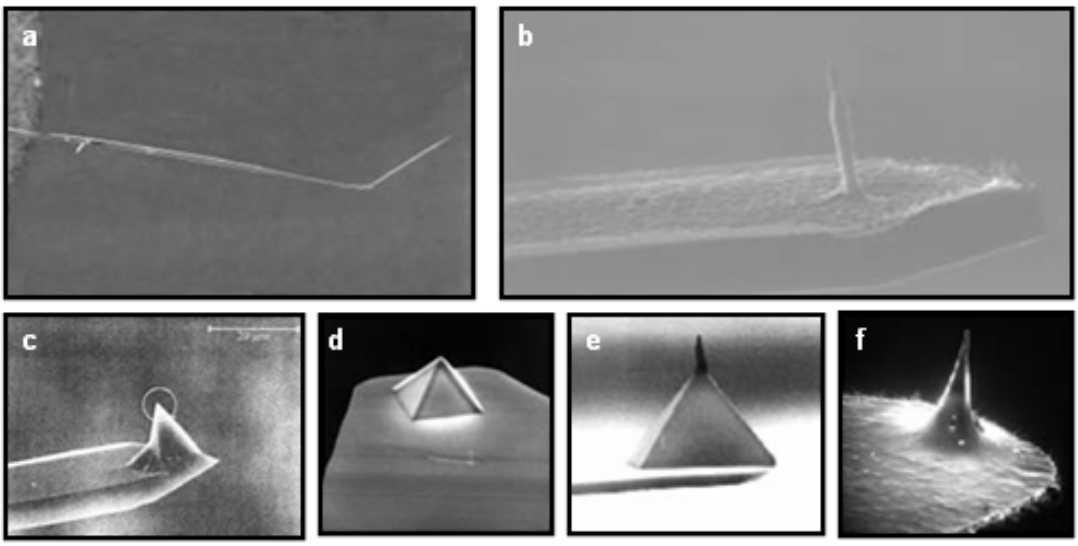

Figure 2.6: *SEM images of different tips, (a) Wire cantilever, fabricated by electrochemical etching and bending, (b) Microfabricated Si cantilever with integrated tip (Albrecht 1990), (c) Electron-beam deposited "supertip" on top of an ordinary Si probe, (d) normal tip (3 µm tall) (Keller 1992), (e) supertip, (f) Ultralever (also 3 µm tall)(http://www.nanotech-now.com/NanoWorld-release-08262004.htm).*

For Morphology characterization of the sample, high resolution non-conductive silicon tips from NT-MDT Company (www.ntmdt.ru) was used. These tips are with force constant 5.5-22.5 N/m and resonant frequency 190-350 KHz. Figure 2.7 shows this type of tips.

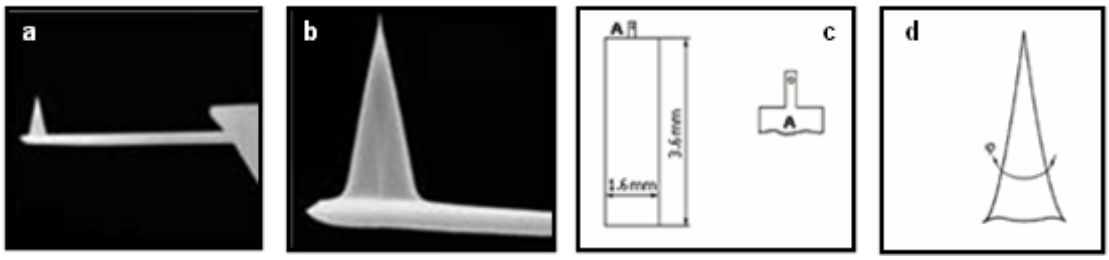

Figure 2.7: *(a)SEM image of NSG10 cantilever holding a tip connected to the holder chip, (b) SEM image of NSG10 tip with height (10 -15 μm), cone angle ≤22^0 and curvature radius of 10 nm,(c) schematic of NSG10 chip and cantilever, (d) NSG10 tip schematic. (http://www.ntmdt-tips.com/catalog/golden/non/products/NSG10_50.html)*

2.1.4 Imaging Modes

The image contrast can be achieved in many ways. The three main operating modes are distinguished on the interaction that they experience. Refer to Figure 2.5, which shows the different modes' operation areas in accordance of the tip-sample force curve. The main three imaging modes are contact mode, non-contact mode and tapping mode.

a) Contact Mode (CM): the contact mode where the tip scans the sample in close contact with the surface is the common mode used in the force microscope. The force on the tip is repulsive with a mean value of 10^{-9} N. This force is set by pushing the cantilever against the sample surface with a piezoelectric positioning element. While the tip scans the surface, the cantilever deflection changes due to the surface profile and a feedback loop maintains a constant cantilever deflection by changing piezo-voltages. The image is obtained displaying the piezo-voltages. Problems with contact mode are caused by excessive tracking forces applied by the probe to the sample. The effects can be reduced by minimizing tracking force of the probe on the sample, but there are practical limits to the magnitude of the force that can be controlled by the user during operation in ambient environments.

b) Non Contact Mode (NCM): in this mode the tip hovers 50 - 150 Angstrom above the sample surface without touching it. Attractive Van der Waals forces acting between the tip

and the sample are detected, and topographic images are constructed by scanning the tip above the surface. The image is obtained keeping the amplitude of the detected force since the tip-sample height is changed in accordance of the feedback signal constant. Unfortunately the attractive forces from the sample are substantially weaker than the forces used by contact mode. Therefore the tip must be given a small oscillation so that AC detection methods can be used to detect the small forces between the tip and the sample by measuring the change in amplitude, phase, or frequency of the oscillating cantilever in response to force gradients from the sample.

The advantage of this mode is that it causes less damage to soft samples. While the disadvantages includes lower scan speed than contact mode and lower lateral resolution.

c) Tapping mode: which is a key advance in AFM that overcomes the limitations of the previous two modes, this technique allows high resolution topographic imaging of sample surfaces that are easily damaged, loosely hold to their substrate, or difficult to image by other AFM techniques. Tapping mode overcomes problems associated with friction, adhesion, electrostatic forces, and other difficulties that an plague conventional AFM scanning methods by alternately placing the tip in contact with the surface to provide high resolution and then lifting the tip off the surface to avoid dragging the tip across the surface. Tapping mode imaging is implemented in ambient air by oscillating the cantilever assembly at or near the cantilever's resonant frequency using a piezoelectric crystal. The piezo motion causes the cantilever to oscillate with a high amplitude (typically greater than 20nm) when the tip is not in contact with the surface. The oscillating tip is then moved toward the surface until it begins to lightly touch, or tap the surface. During scanning, the vertically oscillating tip alternately contacts the surface and lifts off, generally at a frequency of 50,000 to 500,000 cycles per second. As the oscillating cantilever begins to intermittently contact the surface, the cantilever oscillation is necessarily reduced due to energy loss caused by the tip contacting the surface. The reduction in oscillation amplitude is used to identify and measure surface features.

When the tip passes over a bump in the surface, the cantilever has less room to oscillate and the amplitude of oscillation decreases. Conversely, when the tip passes over a depression, the cantilever has more room to oscillate and the amplitude increases.

Tapping Mode inherently prevents the tip from sticking to the surface and causing damage during scanning. Unlike contact and non-contact modes, when the tip contacts the surface, it has sufficient oscillation amplitude to overcome the tip-sample adhesion forces. Also, the surface material is not pulled sideways by shear forces since the applied force is always vertical. Another advantage of the Tapping Mode technique is its large, linear operating range, i.e large scanning area. This makes the vertical feedback system highly stable, allowing routine reproducible sample measurements.

2.1.5 Image Interpretation

One of the most important factors influencing the resolution which may be achieved with AFM is the sharpness of the scanning tip, as well the deformability of the object, and the smoothness of the substrate (Ding 2006). The best tips may have a radius of curvature of only around 5nm. The need for sharp tips is normally explained in terms of tip convolution; Which can be defined as in the case, when the radius of curvature of the tip is comparable with, or greater than, the size of the feature trying to be imaged. Figure 2.8 illustrates this problem; as the tip scans over the specimen, the sides of the tip make contact before the apex, and the microscope begins to respond to the feature.

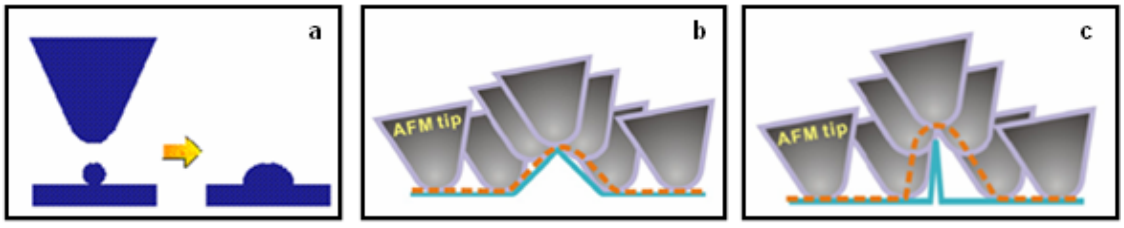

Figure 2.8: *Tip convolution effect on the imaged objects, (a) small objects imaged with a size relative to the tip, (b) topographic image (orange line) contains the shapes of both the tip and the surface and (c) topographic image shows exactly the shape of the tip by imaging a relatively small object(Ding, 2006).*

2.2 Electrostatic Force Microscopy via AFM

2.2.1 Principle

The Electrostatic Force Microscope is a modified AFM where the conductive cantilever is connected to an independently controlled bias. The bias is used to create an electrostatic field between the tip and the substrate. It is intuitively obvious that the size and form of the tip is expected to be a crucial factor limiting the detection and observation of images. In contrast to traditional atomic force microscopy (AFM) which relies on the van der Waals forces, EFM measures the long range Coulomb interaction between a conducting tip and the sample surface, in addition EFM can be used to distinguish conductive and insulating regions in a sample (Jespersen 2005).

The EFM operation of a scanning probe microscope (Figure 2.9) is a dual scan technique where the topography of each scan line is first obtained by standard tapping mode AFM. In the second scan the topographic data is used to retrace the first line with a constant tip-sample separation *h*. In the second scan the cantilever is oscillated at its free resonant frequency and the EFM signal is the phase difference between the driving force and the actual oscillation of the tip (Staii 2001).

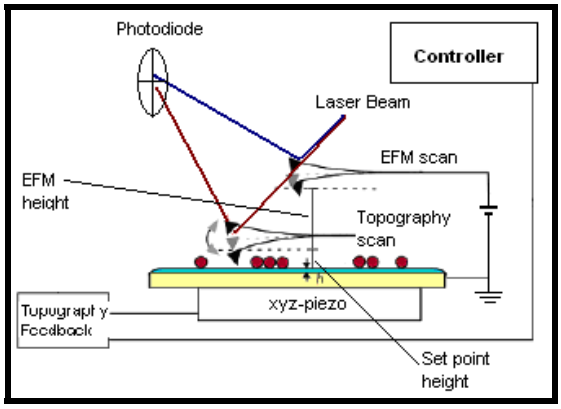

Figure 2.9: *EFM schematic setup*

In a case when a conductive AFM probe is electrically connected to a conductive substrate, creating a capacitor. Spatial variations in the surface charge and dielectric properties create a contrast in the electrostatic forces experienced by the probe. The forces can be separated into two parts: Columbic forces due to static charges and multipoles (F_{coul}) and capacitive forces due to surface potential and dielectric screening (F_{cap}), where EFM force (F_{EFM}) can be written as the algebraic summation of F_{coul} and F_{cap} as follows (Cherniavskaya 2003):

$$F_{EFM} = F_{cap} + F_{coul}$$

$$F_{EFM} = \frac{1}{2}\frac{dC}{dz}V^2 + E_z Q_{tip}$$

where *Ez* is the z-component of the electric field that is due only to the charges and/or multipoles on the surface, where V is the voltage applied between the surface and the probe and *dC/dz* is the derivative of the empty probe-substrate capacitance with respect to *z*, the separation of the probe apex from the conductive plane of the substrate, where local dielectric properties, which affect *dC/dz*, are determined by fitting the measured component of the force gradient at 2ω (Nirmal 1999). Q_{tip} is the sum of the charge on the capacitor CV_{tot} plus the image charges Q_{im} induced by the static charge distribution on the surface, where Q_{tip} is determined from the measured force gradient on the tip at ω (Krauss and Brus 1999). If the total voltage drop between the probe and the surface is $V_{tot} = \varphi + V_{dc} + V_{ac}\sin(\omega t)$. Then one can find that EFM force can be divided into three types of force terms, which are a static term, a term whose amplitude oscillates at the frequency of the applied voltage ω, and a term whose amplitude oscillates at twice that frequency, 2ω (Cherniavskaya 2003). We can write the amplitudes of the force components at ω and 2ω as

$$F(w) = \frac{dC}{dz}(V_{dc} + \varphi)V_{ac}$$

$$F(2\omega) = \frac{1}{4}\frac{dC}{dz}V_{ac}^2$$

Using suitable electronics setup, $F(w)$ and $F(2\omega)$ can be measured and recorded, these two recorded signals corresponding to the phase and dielectric images, respectively. These two types of images are the EFM images that show the electrical behavior sample surface.

2.2.2 Interpretation of the EFM image

The EFM signal is a measure of the force between the tip and the sample surface in the electrostatic range, this force can be repulsion or attraction according the sample and tip charges. In the case of the polarized surfaces the tip-sample force is always attraction, since the voltage on the tip trigger the opposite charge in the sample to be near to the surface. In the case of the charged objects, tip-sample force has two possibilities, if the sample has the same polarity as the tip then the force is repulsion, and if tip has different polarity the force is attraction.

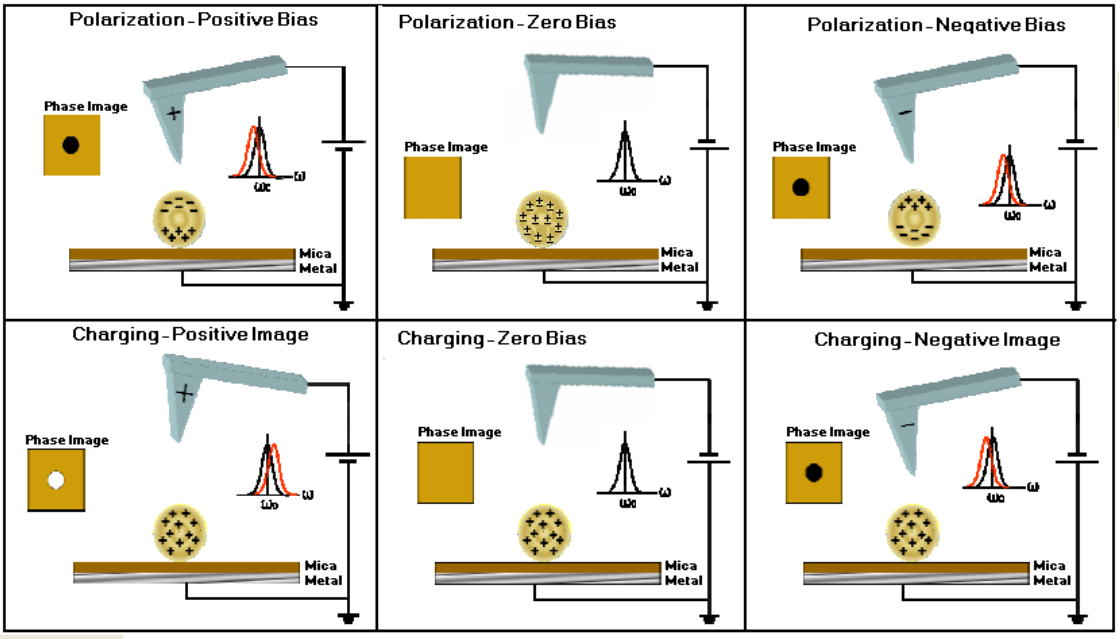

Figure 2.10: *Schematic of the EFM "plane mode" operation. A conductive tip is connected to a conductive surface thus creating a capacitor like setup. The sample is placed between the tip and the conductive surface on a non-conductive material (e.g.,*

mica).Following a topography imaging the tip is raised above the vander Waals range where electrostatic forces are dominant. The AFM feed-back is disconnected and a phase image is acquired. The image shows the phase shift between the inducing and the actual cantilever oscillation frequencies. An attraction between the tip and the sample is accompanied by a decrease in the resonance frequency (black dot in the phase image) and repulsion leads to positive phase shift (white dot in the phase image). In the case of polarization the phase shift is negative for both positive (a) and negative (c) voltages on tip, whereas for charging phase shift is positive (white) for similar charges (d) and negative for opposite charges (f) on tip and measured object. There is no observed signal for zero voltage on tip (b,e).

2.2.3 EFM Modes

a) Plane Mode: Plane Scan is a useful way to measure long range forces which are the electrostatic forces. Long-range forces are detected at much longer distances than Van der Waals forces. This last interaction is the one felt by the tip to do the feedback cycle. If one wants to go far enough to measure the long-range forces, then one cannot use the usual feedback system to control the scan. Plane Scan measures the actual plane of the topography and records it, and uses it to make the tip go over the sample at a distance high enough to measure the long-range forces.

b) 3D Mode: 3D mode is a new way of acquiring data. We usually measure a determined property of the sample over a given area of it. In this case, the horizontal direction would be what we call the fast channel, the vertical direction would be the slow channel and the property measured would be the one represented as an image. Using 3D modes we can select some completely different fast and slow channels, such as voltage, frequency or z position.

When performing a usual scan, you can change to 3D modes. Let´s say that one chooses the Bias/X-Y option for the fast and slow channels, respectively. Then the scan will be performed only above one line (which will be the one above which the tip was moving

when the 3Dmodes was connected). Each time the tip moves forward one point, the bias voltage is varied a quantity that depends on the parameters set by the user. The magnitude we have selected will be measured under these conditions of position and voltage.

High resolution silicon tips with Pt conductive coating brought from NT-MDT Company (www.ntmdt.ru) that were used for EFM imaging, the used cantilevers are with force constant 1.1 N/m and resonant frequency 90KHz.

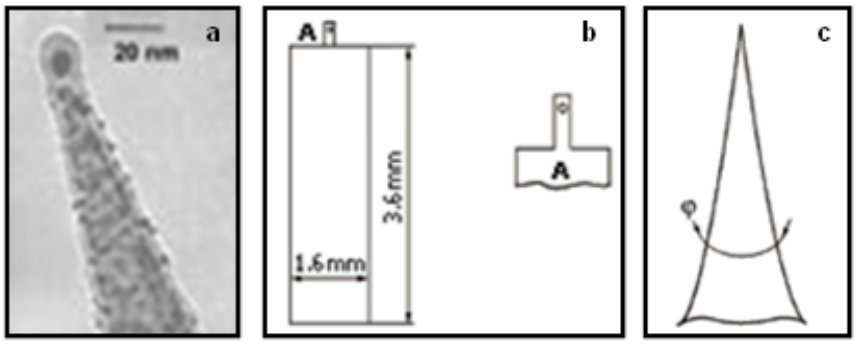

Figure 2.11: *(a) SEM image of NSG03/Pt tip with height (10 -15 µm), cone angle ≤22^0 and curvature radius of 35 nm,(c) schematic of NSG10 chip and cantilever, (d) NSG10 tip schematic. (*http://www.ntmdt-tips.com/catalog/golden/cond/non/pt/products/NSG03_Pt_15.html*)*

2.3 Force Distance Curves (FZ) via AFM

FZ technique is used to measure the tip-sample distance and analyze the long range attractive or repulsive forces between the probe tip and the sample surface, surface contaminants' viscosity, lubrication thickness, elucidating local chemical and mechanical properties like adhesion and elasticity, and even bond rupture lengths.

Force vs. distance (FZ curves) is a record of the vertical force felt by the cantilever as the probe tip is brought close to - and even indented into - a sample surface and then pulled away, or in other words it is a plot of the deflection of the free end of the cantilever versus the vertical extension of the piezoelectric scanner towards and then away from the sample surface, the deflection is measured using a position-sensitive photodetector. This is achieved by applying a triangle-wave voltage pattern to the electrodes for the z-axis

scanner, which causes the scanner to expand and then contract in the vertical direction, generating relative motion between the cantilever and sample. The deflection of the free end of the cantilever is measured and plotted at many points as the z-axis scanner extends the cantilever towards the surface and then retracts it again.

Resulting distances from FZ-curves may change from one case to another, but in all cases they should be in the van der Waals force range which is a range of few nanometers to tens of nanometers. The changes in the tip-sample distances are due to changes in the force constant of the tip, free amplitude applied on tip and set point value, which is the constant force felt by the tip and accordingly tip height is changed to keep it fixed.

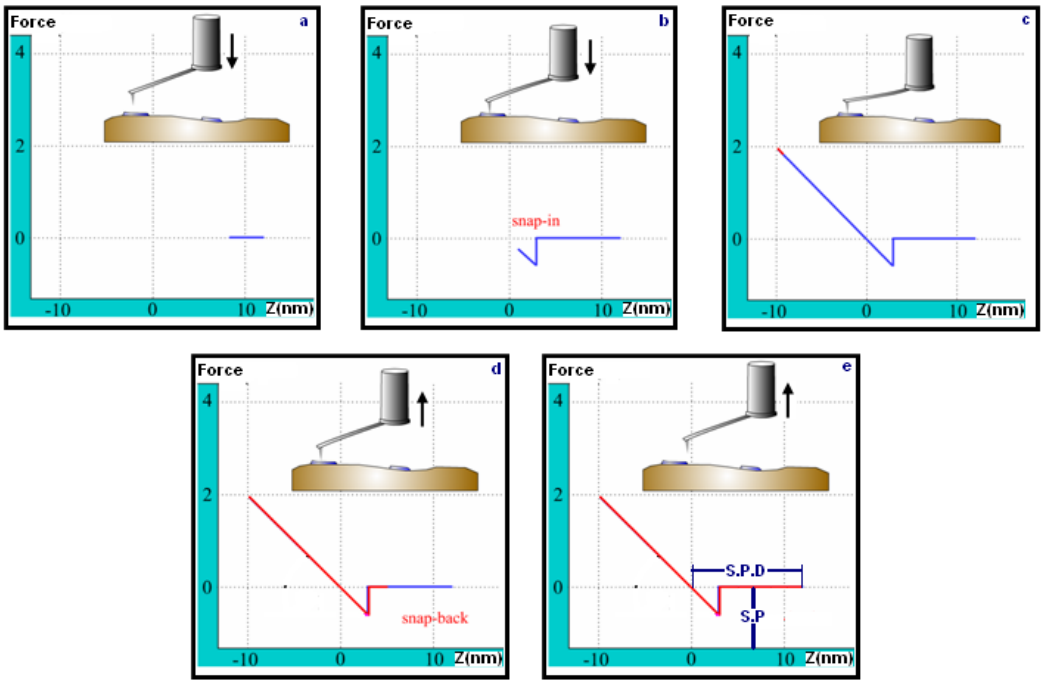

Figure 2.12: *F-Z Technique setup (a) tip is approached gradually to the sample surface while it feels long range force before making contact with the surface, (b) as the probe tip is brought very close to the surface, it may jump into contact if it feels sufficient attractive force from the sample, (c) once the tip is in contact with the surface, cantilever deflection will increase as the fixed end of the cantilever connected to the scanner is brought closer to the sample. If the cantilever is sufficiently stiff, the probe tip may indent into the surface at this point, (d) after loading the cantilever to a desired force value, the process is reversed. As the cantilever is withdrawn, adhesion or bonds formed during contact with the surface may cause the cantilever to adhere to the sample some distance past the initial*

contact point on the approach curve (e) after the tip become free of the adhesion or bonds formed during contact with the surface, it completes withdrawing until return to its normal position. For all schematics, the blue and red curves are the FZ curves acquired.

2.4 Materials

SP1 (Stable Protein 1)

SP1, a stress-responsive, homo-oligomeric protein is isolated from aspen plants (Wang, 2002). It represents a novel family of molecular chaperones, forming an extremely stable oligomer that is resistant to high temperatures, high levels of ionic detergent and various proteases (Wang 2002 and Levy 2002). SP1 is a 12.4 kDa protein with no cystein or glycosilation site. Analytical ultra-centrifugation, chemical cross-linking and matrix-assisted laser-desorption time-of-flight mass spectrometry revealed that SP1 is a dodecamer, while electron microscopy and X-ray crystallography studies revealed that SP1 is an 10 nm in diameter ring-like protein with a 4 nm central cavity.

The SP1 molecule consists of 12 identical protein subunits (12.4 kDa each), which spontaneously assemble into a uniform ring-like shape (10 nm diameter and 2.5 nm width) with a central cavity (4 nm diameter) as shown in figure 2.13 (Wang 2003), which can be modified and adjusted by using genetic engineering to mutate the N-termini that exposed to the central cavity.

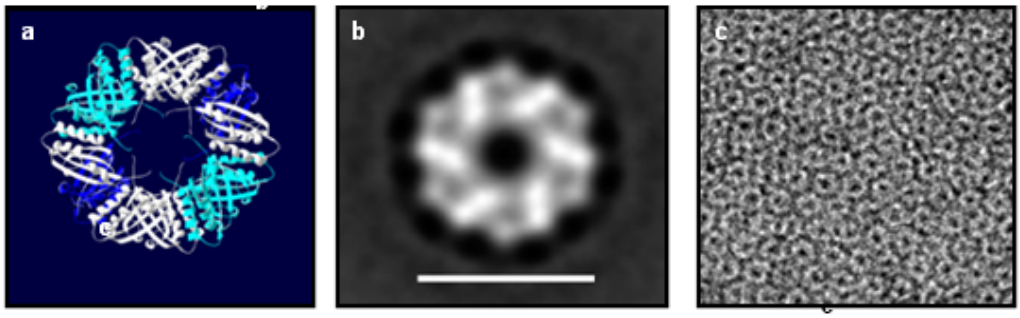

Figure 2.13: *(a) 3-D structure of an SP1 dodecamer elucidation from X-ray crystallography "Utrecht University-Utrecht, the Netherlands" (b) Electron microscopy of SP1 stained with uranyl-acetate. Average of 313 top-view aligned particles (scale bar 10 nm). (c) SP1-protein array prepared by the water/phospholipid coating method and observed with TEM. "Electron Microscopy Unit, Weizman Institute of Science, Rehovot-Israel"*

The N-termini of SP1 are pointing from the central cavity to the opposite planes of the ring, in a way that 6 N-termini point to one side and the other 6 N-termini point to the opposite side as presented in figure 2.14. Therefore, cystein groups at the N-termini of SP1 dodecamer will enable the binding of the SP1 ring in a flat orientation to the gold surface underneath and to the gold nanoparticle at the center on top of the SP1 ring.

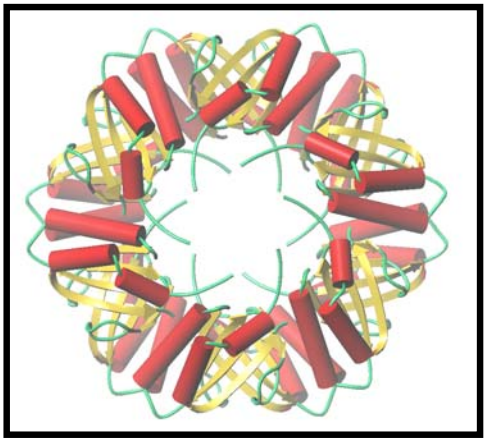

Figure 2.14: *Crystal structure of an SP1 dodecamer showing the N-termini of SP1 pointing from the central cavity to the opposite planes of the ring, in a way that 6 N-termini point to one side (perpendicular into the screen) and 6 N-termini point to the opposite side.(perpendicular out of the screen) (Wang 2003).*

SP1 protein that is used in the experiment is an initial protein specimen was dissolved in a proper deionized water to obtain a solution with concentration of 0.5 µg/ml, this solution were purchased from fulcrum SP1 Ltd, at Herzliya, ISRAEL

Gold Nano-particles

The study of gold nanoparticles is very important in the field of nanomaterials because they have many potential applications. For example, they could serve as the basis for new technologies that will render obsolete the energy intensive methods currently used to fabricate computer semiconductors (Tanaka, 1999). Gold nanoparticles having purchased size ranging from 2 to 110 nm (Tapan 2001).

The gold nano-particles solution used is of 1.8 nm in dimension and concentration of 2 % (w/v) in toluene and density of 0.8737 g/mL at 25 °C, this solution was purchased from sigma-Aldrich Ltd.

Mica

At present time available AFM substrates for SP1 imaging are limited in types; the conventional support for the biological objects is mica (Hansma 2000).

Mica is hydrous silicates of aluminum and potassium, often containing magnesium, ferrous iron, ferric iron, sodium, and lithium and more rarely are containing barium, chromium, and fluorine. All crystallize in the monoclinic system, but mica is most commonly found in the form of sheets and can split into very thin, elastic laminae (James 1999). The entire mica surfaces can be easily updated by a simple cleaving, by first pressing some adhesive tape against the top mica surface, then peeling off the tape. Some varieties are transparent; resistant to heat. Commercially, the most important micas are muscovite (potassium mica) and phlogopite (magnesium mica). Muscovite, the commoner variety, is usually colorless, but it may be red, yellow, green, brown, or gray.

Thin mica sheets with dimensions of 1 cm^2 used in the experiment were purchased from SPI supplies, USA.

Deoxyribonucleic acid (DNA)

5'-thiolated 22bp ssDNA (Thiol 5'TAACAGGATTAGCAGAGCGAGG3') and its complementary strand, and 5'-thiolated 80bp ssDNA (5'TAACAGGATTAGCAG AGCGAGGAATCATACGTACTCAACTGCTGGGAGCGAGACGATTAGGACAATA ACTTGGTATGCT3') and it's partially complementary strand were purchased from Biomers Company (http://www.biomers.net). The sequence of the 80bp ssDNA was designed to partially anneal to its partially complementary strand leaving sticky ends capable of annealing to non annealed end of the other strand, see fig 4.4 for illustration.

Chapter THREE

Architecture of SP1 protein-Gold nanoparticle based Nanoelectronics devices

Chapter THREE

Architecture of SP1 protein-Gold nanoparticle based Nanoelectronics devices

3.1 The Basic Building Block

A Gold nanoparticle 1.8 nm in diameter is attached to the central cavity of the ring shaped SP1 protein (outer diameter 10nm, inner diameter 4nm, and height 2.5nm) to form a building block, i.e unit cell, then these unit are attached to each other "in a Lego like fashion" to form more complicated structures like nanowires and 2 D arrays that serves as ultra high density memory.

Assembling GNP in the central cavity of SP1 is done without guidance or management from an outside source, this process is known as self-assembly. "Self-assembly is a manufacturing method used to construct devices at the nanoscale, which is comprised of structures with at least one dimension that is less than 100 nano's. In self-assembly the final (desired) structure is 'encoded' in the shape and physical, chemical and electrical properties of the molecules that are used, as compared to traditional techniques, such as lithography, where the desired final structure must be carved out from a larger block of matter (Boncheva 2002). Self-assembly is thus referred to as a 'bottom-up' manufacturing technique, as compared to lithography being a 'top-down' technique" (Quintarelli 2006).

Genetic engineering was used to add six-histidine tag to the N-terminal of the SP1, in order to enable the binding of the 1.8 nm Ni-NTA GNP to the center of the dodecamer. The diameter of the Ni-NTA GNP's, 1.8 nm, fits well into the diameter of the dodecamer's inner pore, which is about 4 nm. The interaction of Ni-NTA and the histidines causes the GNP binding in the central cavity of the SP1.

The SP1-GNP hybrid is shown schematically in figure 3.1 and is imaged with high-angle annular dark-field scanning transmission electron microscopy (HAADF-STEM) in figure 3.1(d-f). The top views figure 3.1(d,e) show the gold (bright white contrast) to be centered

within the darker round particle. The side views (f) show that both sides of the dodecameric ring have gold attached to them, which is consistent with the crystal structure, since there are six N-termini on each face.

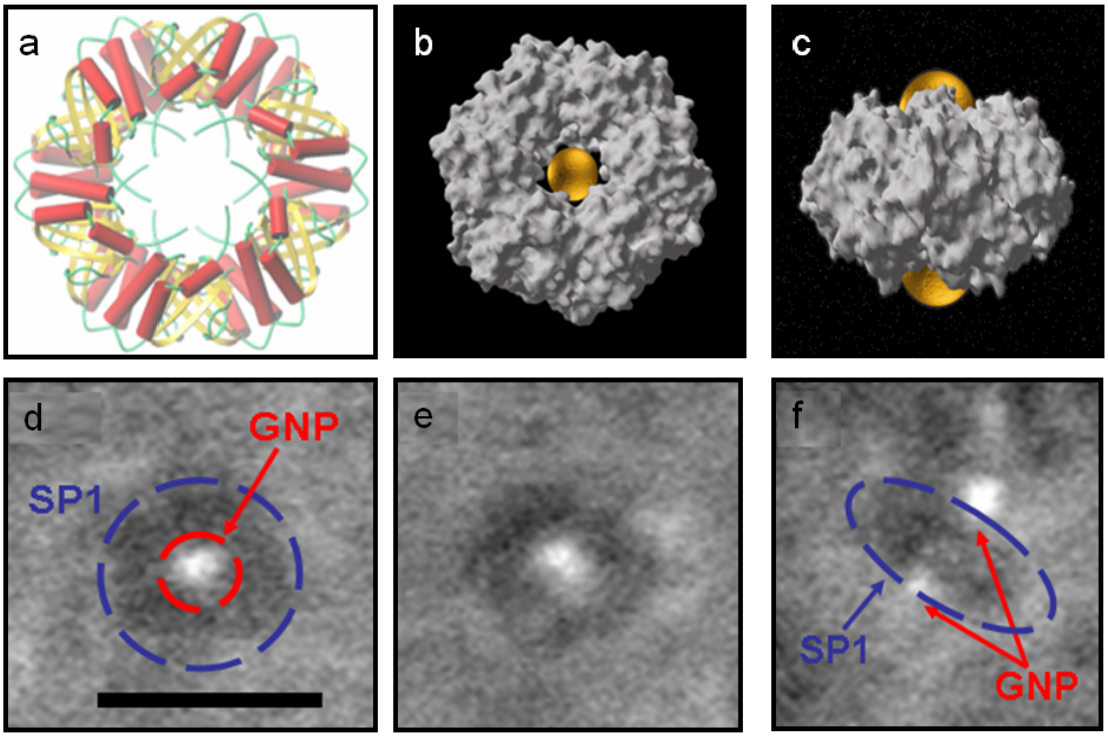

Figure 3.1: *(a) Crystal structure of an SP1 dodecamer showing the N-termini of SP1 (b,c) A computer simulation of the hybrid in a top and side views. (d-f) HAADF-STEM images of two top views (d,e) and side view (f) of the SP1-GNP hybrid (scale bar: 10 nm) "Electron Microscopy Unit, Weizman Institute of Science, Rehovot-Israel".*

3.2 Possible nano-Electronic Devices Architecture

3.2.1 Molecular wire

DNA oligos were designed to form either short or very long DNA wires. In case of short wires, fully complementary 22bp DNA were purchased. To have longer wires, partially complementary 80bp DNA were purchased. To enable binding of the DNA wires to gold nanoparticles, the oligomers were thiolated at the 5' end. To prepare dsDNA, equimolar

concentration (100nM) of sense and complementary antisense oligos were mixed in triple distilled water and annealed in a PCR machine. Mixture was heated to 95 ºC for 4 minutes, then incubated at 70 ºC for 10 minutes, and finally the temperature was decreased to 4 ºC slowly (0.5 ºC/min), and kept at 4 ºC for 10 minutes (Yao 2007). To ensure annealing, samples before and after treatment were analyzed by agarose gel electrophoresis. Only after annealing DNA could be seen in ethidium bromide gel, confirming the formation of dsDNA, figure 3.2. To bind SP1-GNP to dsDNA nanowires, two folds molar excess of SP1-GNP was mixed with dsDNA and incubated at 37 for 3hrs. In the case of Short dsDNA-SP1-GNP nanowires only one option could result; two SP1-GNP linked with 22bp dsDNA wire. In case of long dsDNA-SP1-GNP nanowires, different combinations can result; two SP1-GNP linked with 80bp or its folds dsDNA wire, SP1-GNP on long dsDNA wire separated by 22, 54 or 80bps, or a multi connection of dsDNA with SP1-GNP blocks, see figure 3.4 for illustration.

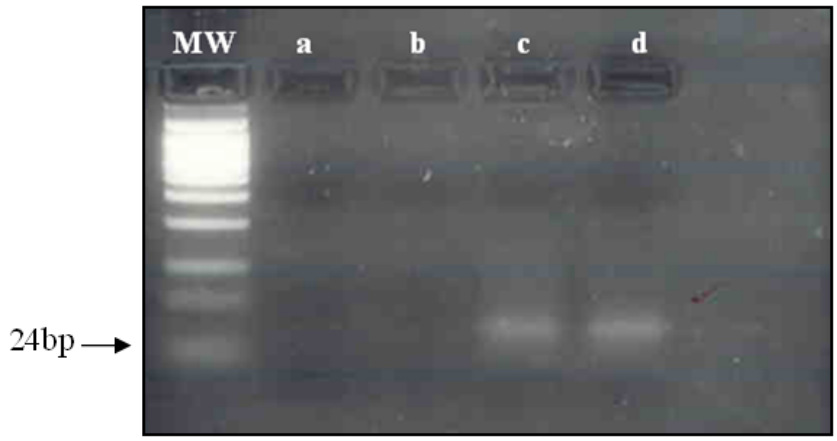

Figure 3.2: *(MW) DNA ladder;phi X 174DNA/Hinf I, (a,b) nonannealed ssDNA, (c,d) annealed dsDNA "Done at Al-Quds University".*

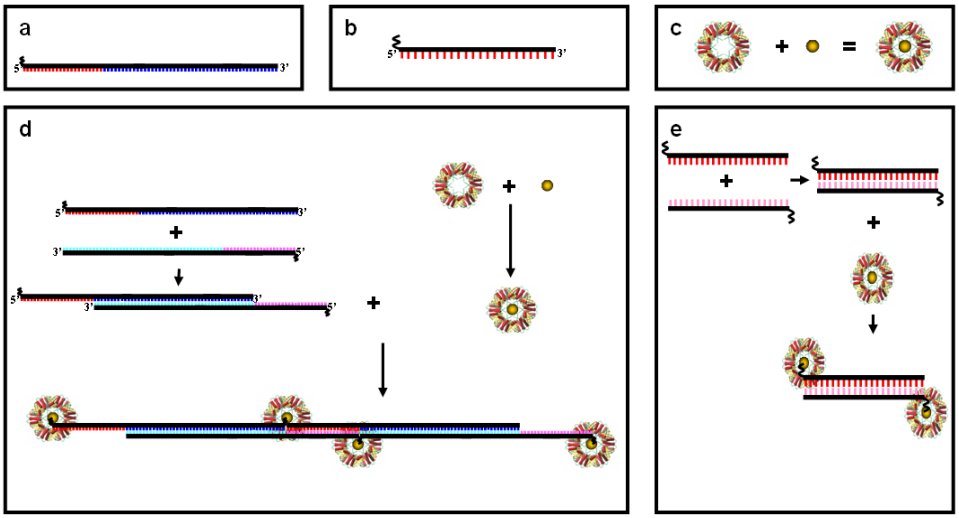

Figure 3.3: *(a) 80bp ssDNA ended with thiol (b) thiolated 22 bp ssDNA, (c) SP1-GNP hybrid, (d) SP1-GNP hybrids connected via long dsDNA (e) SP1-GNP hybrids connected via 22bp dsDNA.*

3.2.2 Ultra High density Memory

The idea behind the high density memory is to form a 2D array of SP1 molecules using a Longmuir-Blodgett technique and assembling a gold nanoparticle in each molecule. A sharp conductive AFM tip will be used to charge, discharge, and polarize the nanoparticles. Figure 3.4 shows the prototype of the memory cell we propose.

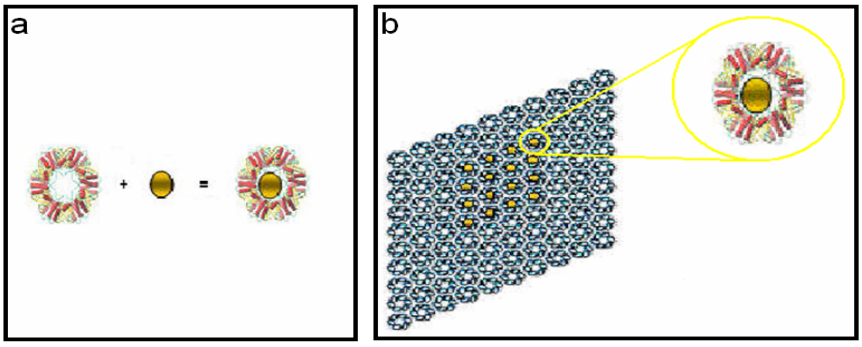

Figure 3.4: *(a) Schematic of SP1-GNP hybrid (b) Schematic representation of the proposed memory cell.*

Chapter FOUR

Results and Discussion

Chapter FOUR

Results and Discussion

4.1 Characterization of SP1 protein

Few micro letters of SP1solution are deposited on cleaved mica, after waiting for suitable incubation time, letting the SP1 solution to spread all over the mica substrate, the prepared sample is flushed with distilled water and dried with nitrogen gas. Through out the experiment, we tried to optimize the following parameters, concentration, incubation time and the amount of SP1 solution on mica to get separate single molecules and not monolayer or aggregate to perform single molecule based experiments. Most reproducible results are prepared with dilution ratio (1 SP1 "Concentration = 0.5 µg/ml ":50 Triple Distilled water), incubation time is 10 minutes.

4.1.1 Morphological characterization of SP1 Molecules

SP1 protein deposited on Mica surface was characterized using tapping mode AFM. Figure 4.1 shows SP1 molecules, and their height profiles, with a histogram image shows the SP1 molecules heights distributed in the range 2.2nm to 2.8 nm.

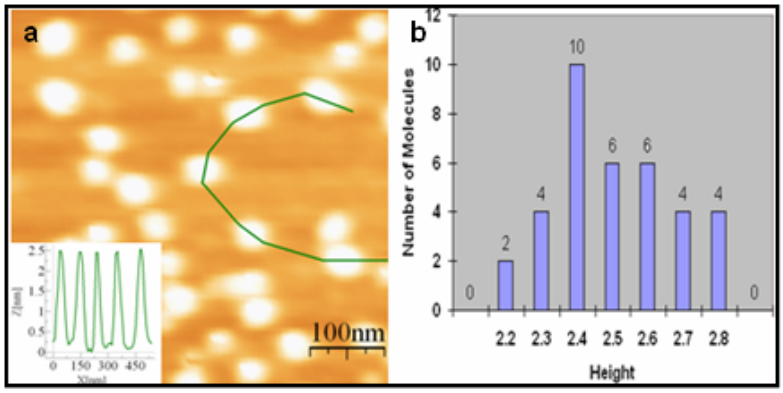

Figure 4.1: *(a) AFM Topography images of SP1protein without gold-nanoparticle acquired in tapping mode, (insert) cross section showing the height of SP1 molecules (c) histogram shows SP1 molecules heights distribution "Acquired at Nanotechnology Research Laboratory - Al-Quds University".*

From the FZ-curves that are in figure 4.2, the tip-surface distance is found to be in the range (51nm ±2nm), the tip-surface distances differences are according to apply bias voltage on tip. Figure 4.2 shows the acquired FZ-curves for zero and +/-5V bias voltage,

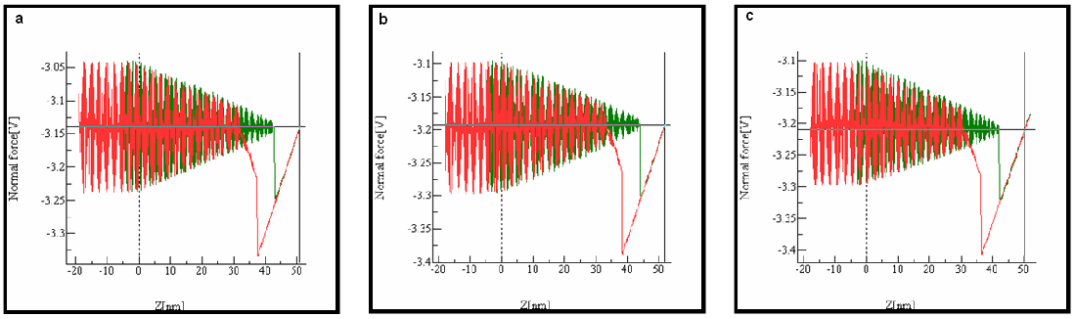

Figure 4.2: *FZ-curves for SP1 complex with (a) zero bias voltage (Sample-tip distance = 50.7nm), (b) +5 bias voltage (Sample-tip distance = 51.2 nm), (c) -5 bias voltage (Sample-tip distance = 50.5 nm) "Acquired at Nanotechnology Research Laboratory - Al-Quds University".*

I found that the concentration and the incubation time does not affect the characteristics of the SP1 protein rings, in all cases the average height of the protein is (2.5 nm ± 0.25 nm) as appears in the figure 4.1. Also the tip-sample distance is not affected by changing the SP1 complex concentration or incubation time.

4.1.2 EFM Images

To perform an electrostatic force microscopy measurement, the tip is lifted and the phase shift between the derived signal on the tip and the actual tip position estimated via laser signal is measured in volt with disconnected feedback at lifted height that I choose in the range (10 nm – 18 nm), with various bias voltages applied to the tip, so surface electrical properties is investigated and polarizable, charged and insulator regions are determined.

From the EFM results, figure 4.3, we see that there is no indication for electrical response. In fact, the EFM images give a proof that SP1 protein has no polarizability, since there is no electrical response appears in the EFM images when we change the bias voltage.

Where tip-sample distances 65.7 nm, 66.7 nm and 56.5 nm respectively (lift distance equals 15 nm). These images are shown in figures 4.3.

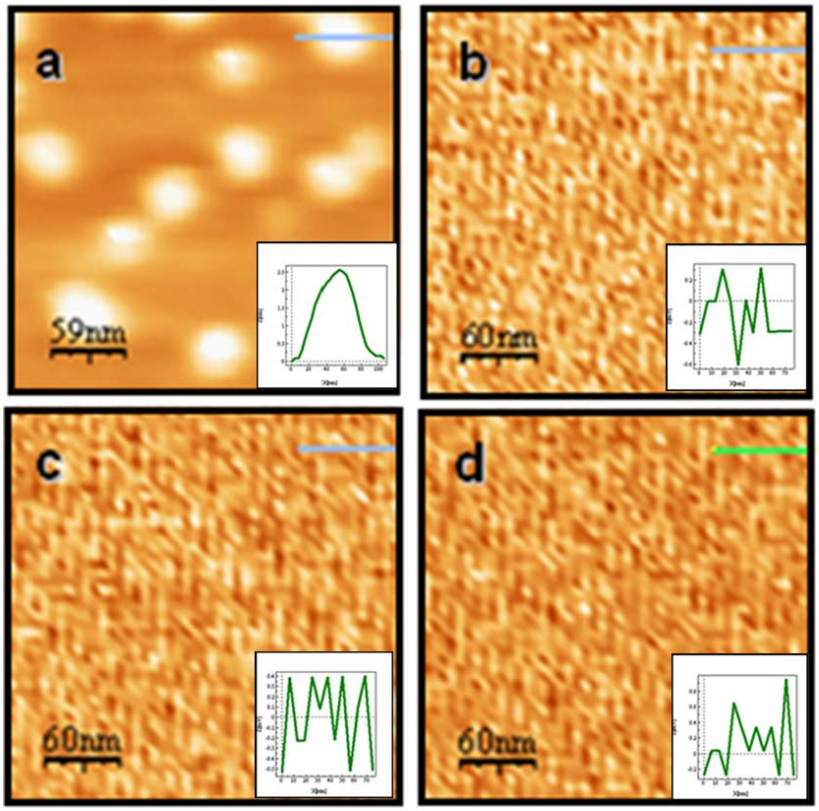

Figure 4.3: *(a) AFM topography image of SP1 molecules without GNP, "insert" cross section shows the height of SP1 molecule indicated on topography image, (b,c,d) Phase images for the area recorded in (a) with various bias voltages applied to the tip +5V, 0V and -5V respectively, "insert" cross section shows the phase shift in volts "Acquired at Nanotechnology Research Laboratory - Al-Quds University".*

4.2 Characterization of SP1-GNP Hybrids

Gold nanoparticles of radius 1.8 nm and concentration of 2 % (w/v) in toluene and density of 0.8737 g/mL are added and mixed carefully with SP1 solution of concentration 0.5 µg/ml, the resultant solution allowing self-assembly of gold nanoparticles and SP1 molecules taking place, then the solution is diluted and deposited on mica substrates under the optimized conditions and parameters that SP1 samples are prepared.

4.2.1 Morphological characterization of SP1-GNP Hybrids

Samples are prepared with optimized incubation time and dilution as before. Figure 4.4 shows SP1-GNP hybrids on mica surface.

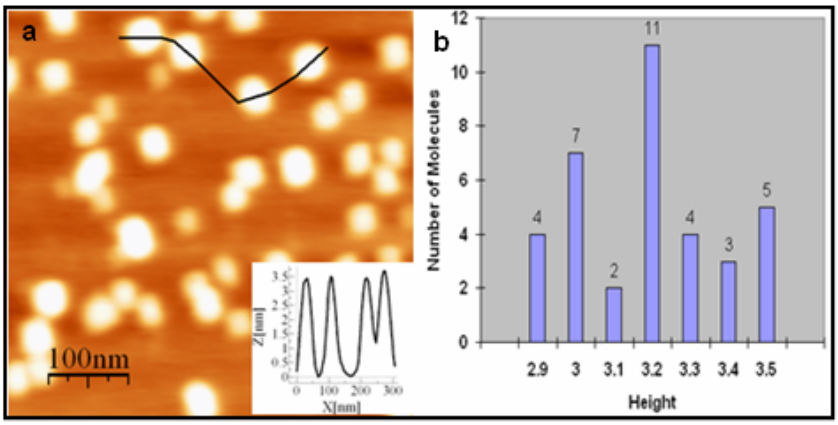

Figure 4.4: *(a) AFM topography image of SP1-GNP hybrid (insert) cross section of height profile of two SP1-GNP units, (b) histogram shows SP1 molecules heights distribution) "Acquired at Nanotechnology Research Laboratory - Al-Quds University".*

High resolution image of SP1 protein-GNP hybrid was obtained using ultra sharp tip, Laplace filter and contour techniques are used to produce images with more details for single SP1-GNP unit, these results are recorded in figure 4.5.

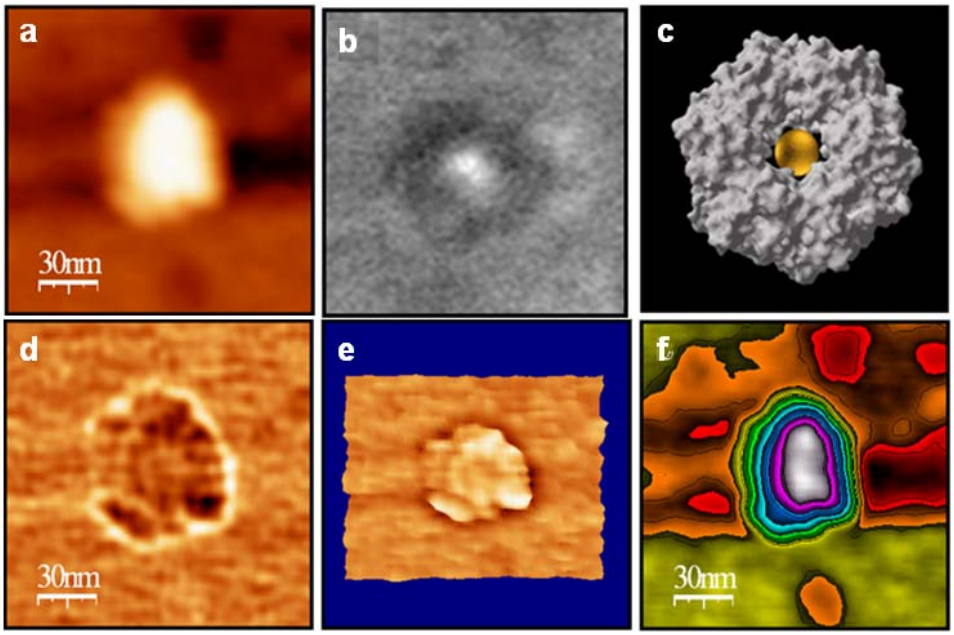

Figure 4.5: *(a) Topography image of single SP1-GNP hybrid, (b) HAADF-STEM images of the SP1-GNP hybrid in a top view, (c) A computer simulation of the SP1-GNP hybrid in a top view, (d) Filtered Image of (a) with Laplace filter, (d) 3D image of the filtered image shown in (d), (f) Contour image for the block shown in (a) "Acquired at Nanotechnology Research Laboratory - Al-Quds University".*

Tip-sample distances curves for the SP1-GNP complex are shown in figure 4.6, for the three bias cases, zero bias and +/-5V. In addition, here there are some small differences in these distances according to changes in bias voltage.

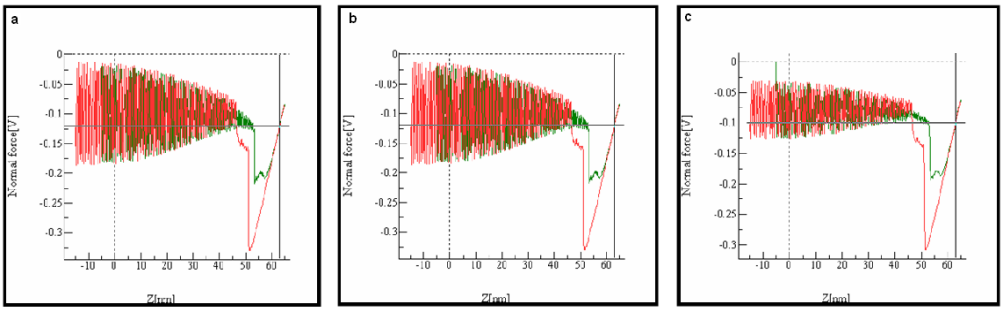

Figure 4.6: *FZ-curves for SP1-GNP complex with (a) zero bias voltage (Sample-tip distance = 63 nm), (b) +5 bias voltage (Sample-tip distance = 62.9 nm), (c) -5 bias voltage (Sample-tip distance = 62.5 nm) "Acquired at Nanotechnology Research Laboratory - Al-Quds University".*

For images in figure 4.4, we see that the height of the SP1-GNP units are in the range of (3.2 nm ± 0.2nm), remember that the SP1 molecule is found to be in the range (2.5 nm ± 0.25 nm). It is evidence from the height difference that GNP's are bonded to the SP1 molecules and the difference in height is due to those GNP.

4.2.2 EFM Images

EFM measurement is performed in the same procedure as for SP1 molecules, and Phase shift images are obtained, here the start-up height (lift distance) is 12 nm, and so the total tip-sample distance is approximately 65 nm.

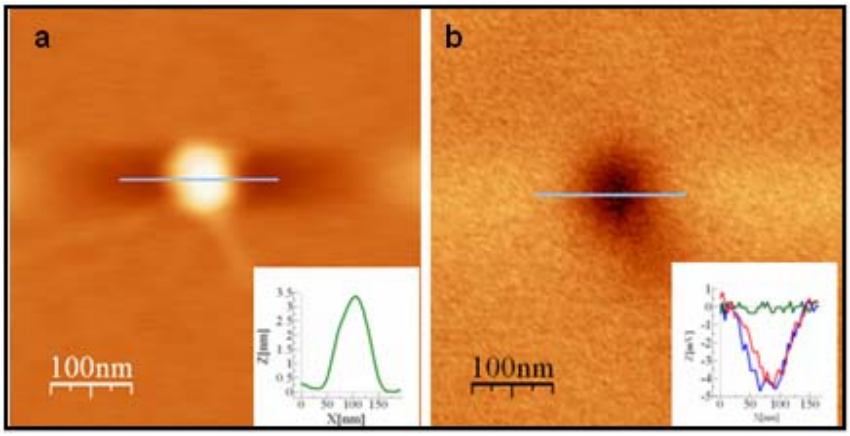

Figure 4.7: *(a) AFM topography image of SP1-GNP unit (insert) cross section shows the height of SP1-GNP unit (b) Phase image of the SP1-GNP unit in (a) with bias voltage +5V (insert) cross section shows the EFM signal on the SP1-GNP indicated in (a), red curve is due to +5V bias, blue curve is due to 0V and green curve is due to -5V bias "Acquired at Nanotechnology Research Laboratory - Al-Quds University".*

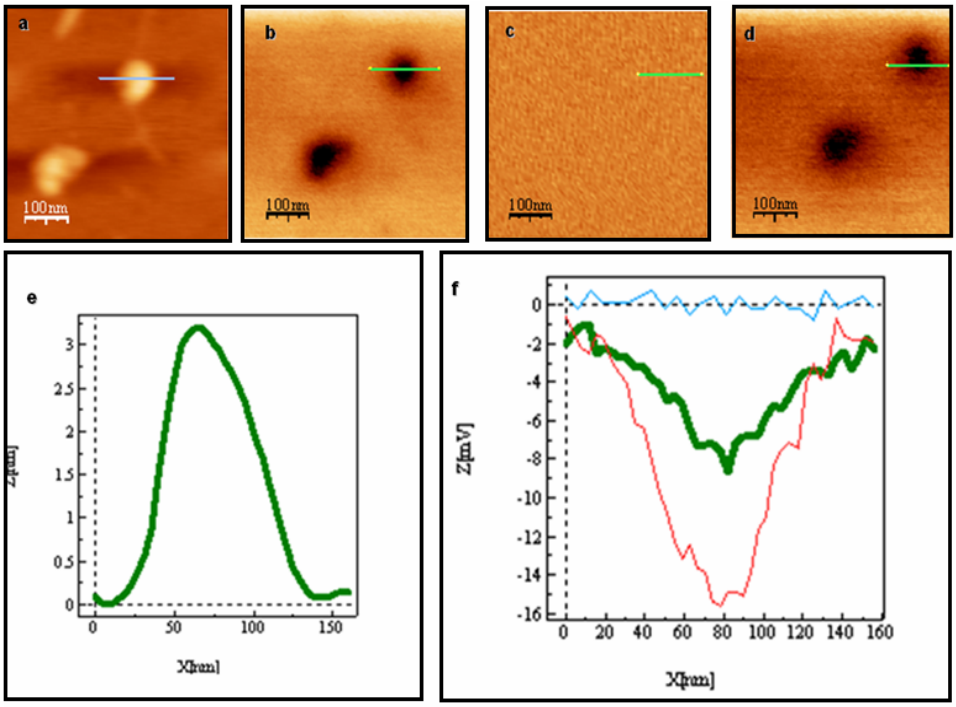

Figure 4.8: *(a) AFM topography image of SP1-GNP units (b,c,d) Phase images of the SP1-GNP units in (a) with bias voltage +5V, 0V and -5V V, respectively (e) cross section shows the height of SP1-GNP unit as indicated in (a) (height 3.2 nm), (f) cross section shows EFM signal on the SP1-GNP indicated in (a), red curve is due to +5V bias, blue curve is due to 0V and green curve is due to -5V bias "Acquired at Nanotechnology Research Laboratory - Al-Quds University".*

Phase images in figure 4.7 and figure 4.8 are for SP1-GNP blocks with bias voltages +5V, 0V and -5V, phase images are recorded when the tip-surface distance is in the range (65.5nm – 66.7nm) these images give an evidence that the SP1-GNP hybrid is polarizable, while figure 4.3 shows that SP1 molecules are not polarizable. So, the SP1-GNP hybrid polarizability is due existence of the GNP in the central cavity of the SP1 protein.

4.3 Ligo like fabrication of nano-electronic devices

4.3.1 SP1-GNP Nano-wires

The SP1- GNP complex is assembled with thiolated DNA molecules as described section 3.2.1. More than one DNA molecule can be attached to the gold nanoparticle depending on three factors: (i) the depth to which the nanoparticle is imbedded inside the central cavity of the ring shaped protein (ii) the size of the nanoparticle (iii) number of gold nanoparticles inside the central cavity of the protein. Figure 4.9 shows AFM results that acquired in tapping mode, these results shows that the DNA is attached to the gold nanoparticles through the thiols.

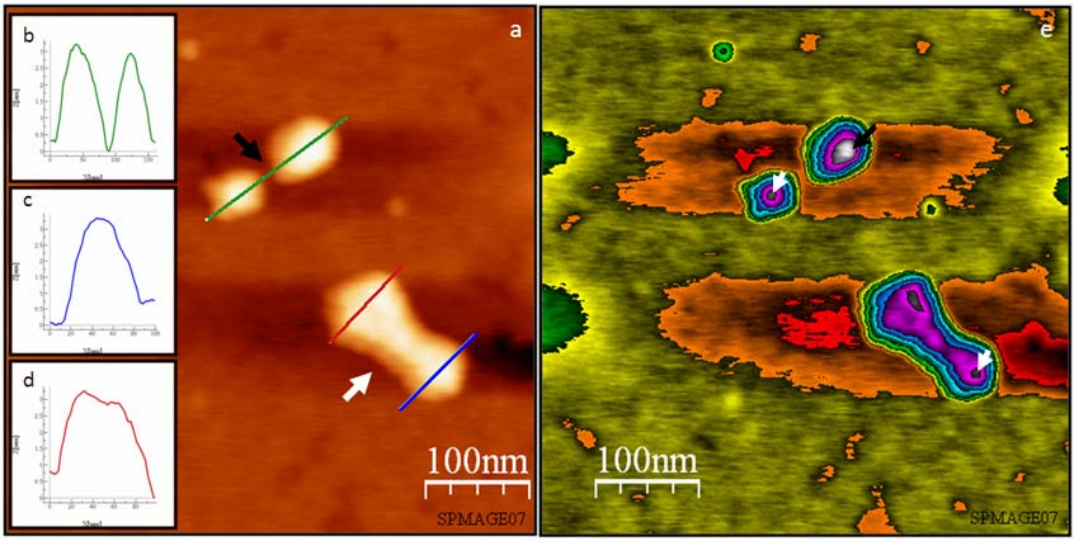

Figure 4.9: *(a) AFM imaging of SP1 with GNP once shown with a dsDNA-ended with thiol connection (white arrow) of 22bp of length and once without (black arrow) (b,c,d insert) Cross sections of height profiles extracted from AFM scanning showing the different heights of the two pairs of SP1-GNP (e) Contour image shows the position of GNP in the central cavity of SP1 "Acquired at Nanotechnology Research Laboratory - Al-Quds University".*

Another striking form of behavior for SP1-GNP and DNA is shown in figure 4.10. AFM images show that a wire-like conduct can be obtained from deposition of the three components of SP1, GNP and thiolated DNA. 80bp thiolated DNA as in figure 3.4 (d) is

used for the same purposes of inter-connecting the SP1-GNP molecules. This AFM image shows the increased spacing between molecules if compared to the distance found between molecules in figure 4.9, where I use a shorter DNA of 22bp. AFM illustrates as well the possibility of connecting the DNA in several parts of the SP1 as shown in the same figure. The distance between the SP1-GNP molecules are as expected in the theoretical analysis.

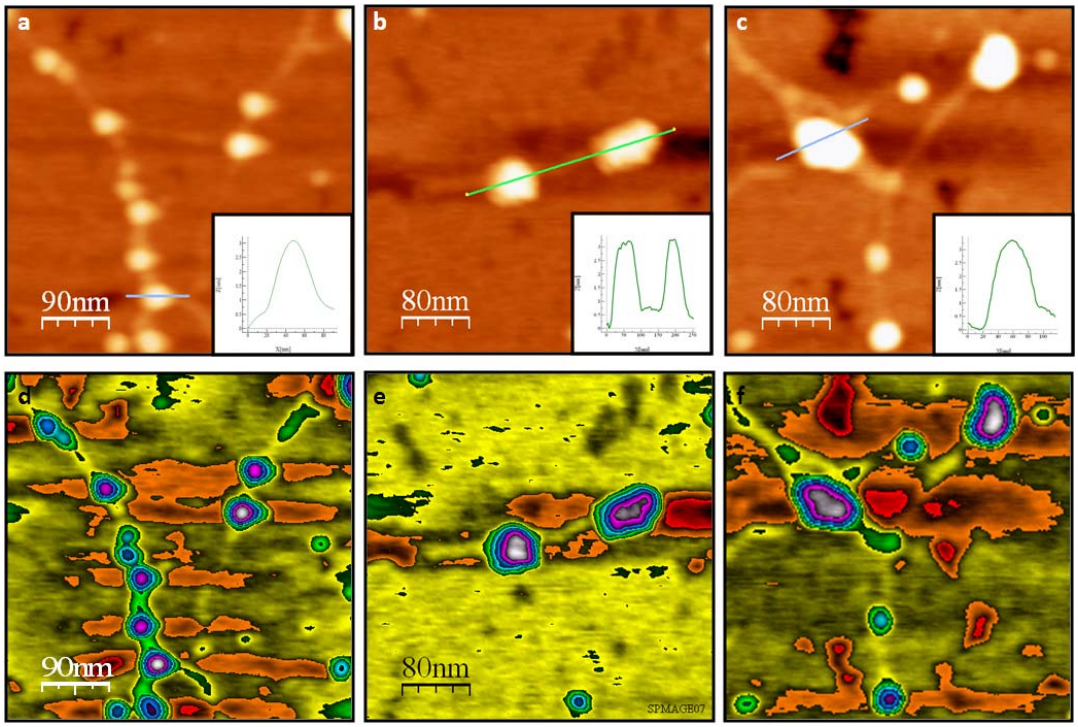

Figure 4.10: *Different examples of SP1-GNP nanowires (a) Topography of SP1-GNP and a dsDNA-ended with thiol group of multi-80bp of length connecting each pair of SP1 (insert) Diagram corresponding to the cross section exposed in the topography image depicting the height of the SP1, (b) Tapping mode imaging of a single connection between a pair of SP1-GNP blocks with ~130 nm as distance in between due to the hybridization of partial complementation of dsDNA (insert) the corresponding height diagram for the shown cross section in (b), (c) Tapping mode imaging of a multi connection of dsDNA with SP1-GNP blocks due to the hybridization of partial complementation of dsDNA (insert) the corresponding height diagram for the shown cross section in (c), (d,e,f) contour images for the topography images (a,b,c)respectively shows the existence of GNP inside SP1 molecules "Acquired at Nanotechnology Research Laboratory - Al-Quds University".*

EFM measurement was carried on the wire that is shown in topography of Figure 4.11 (a). The phase imaging of EFM is shown in Figure 4.11 (c). Polarizability was detected after applying positive and negative biases between the tip and the surface sample. No EFM signal was obtained at zero bias.

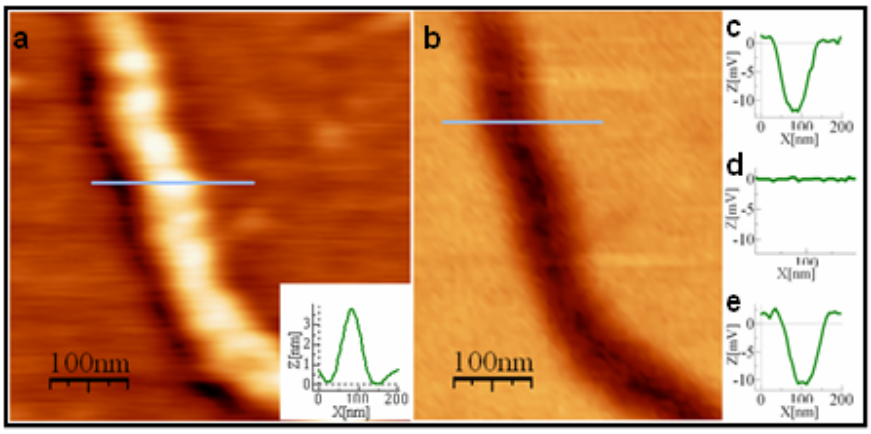

Figure 4.11: *(a) AFM topography imaging of SP1-GNP-DNA forming a wire like behavior (insert) Height diagram corresponding to the cross section shown (b) Phase shift image for an EFM process applied on the same SP1-GNP-dsDNA combination shown in (a)(c,d,e) EFM profiles corresponding to the cross section shown in (b) for +5V, 0V and -5V, respectively. "Acquired at Nanotechnology Research Laboratory - Al-Quds University".*

4.3.2 SP1-GNP Array

SP1 array is produced with Langmuir-Blodgett technique on carbon grid. Langmuir-Blodgett film including a water bath having a spread region for spreading a material on a liquid surface, a compression region for compressing the material spread by the spread region to form a single molecular film, and a lamination region for laminating the single molecular film formed by the compression region on a substrate. So an array of SP1 molecules as shown in figure 4.12 is prepared.

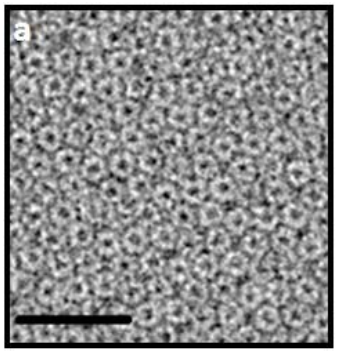

Figure 4.12: *A TEM image of a self-assembled 2D crystalline array of recombinant SP1-GNP molecules formed under a charged lipid layer (dimension bar 60 nm) "Electron Microscopy Unit, Weizman Institute of Science, Rehovot-Israel".*

Unfortunately, the Langmuir-Blodgett technique is not suitable for forming two dimensional array on mica or gold surfaces, we tried to increase the concentration of SP1-GNP complex, promising results as shown in figure 4.13 where obtained and will be continued as future work, this image shows SP1-GNP sub-arrays with their corresponding cross section that shows SP1-GNP heights.

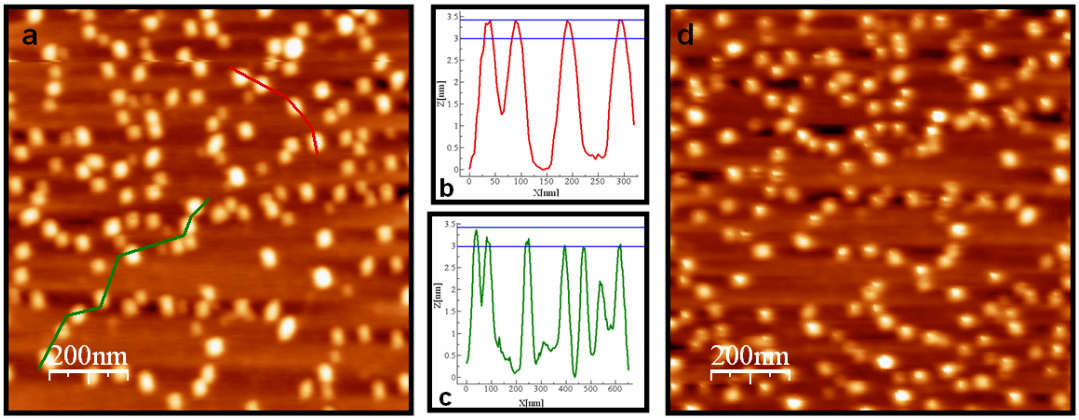

Figure 4.13: *(a,d) AFM topography image of SP1-GNP hybrid acquired with taping mode (b,c) cross section shows heights for SP1-GNP units from images (a), height is in the range (3 nm – 3.4nm) "Acquired at Nanotechnology Research Laboratory - Al-Quds University".*

Chapter FIVE

Conclusion and Future Work

Chapter FIVE

Conclusion and Future Work

5.1 Conclusion

In this work, a basic building block for construction of nanoelectronic devices in a bottom up approach is introduced; this building block consists of gold nanoparticle (1.8 nm in dimension) embedded at the central cavity of a ring protein (outer diameter 10 nm, inner diameter 4 nm and height 2.5 nm). The function of the gold nanoparticle is electron transport, while the function of the protein is a scaffold or a template to position and bind the gold nanoparticle. These building blocks are connected to each other by different mechanisms to form nanowires and 2D arrays.

Tapping mode AFM results shows the height of the SP1 is in the range (2.5 ±0.25 nm), while the SP1-GNP block height is in the range (3.2 ±0.2 nm), which make it a good candidate a nanostructure building. EFM results shows that the bare SP1 molecules are electrically silent while GNP-SP1 hybrids are polarizable, which is a strong evidence of conductivity.

5.2 Future Work

The promising results in this work enhance the following future work;

- To measure real conductivity in the constructed nanowires using electrical transport measurements.

- Development of methods for “writing” and “reading” discrete states in each nanoparticle using a conducting atomic force microscope (AFM) tip and charging effects.

- Attachment conducting and semiconducting nanoparticles in the central cavity of SP1, to construct different nanoelectronic components.

References

References

[Albrecht 1990] Albrecht T. R., Akamine S., Zdeblick M. J., and Quate C. F. (1990). "**Microfabrication of integrated scanning tunneling microscope",** J. Vac. Sci. Technol. V 8, p 317.

[Andrea 2003] Andrea A., Mimmo G., Paolo F., Bernhard S. and Rudiger K., (2003). "Tuning molecular orientation in protein films surface", Science, V **542**, p 64.

[Andrew 2002] Andrew R., Chad P., Jeanie H., Suzanne C., Nestor Z. and Jonathan T., (2002). "Ordered nanoparticle arrays formed on engineered chaperonin protein templates", nature materials, V **1**, p 247.

[Binng 1986] Binng G., Quate C.F. and Greer Ch., (1986). "Atomic Force Microscope". Phys. Rev. Lett. V **56**, p 930.

[Binng 1985] Binng G., Roher H., (1985). "The Scanning Tunneling Microscope". Scientific American, V **74,** p 50.

[Brain 2001] Brain R., Jermiah M., Benjamin M., Michael N. and Christine K., (2001). "DNA-Direct assembly of antistrophic nanoparicles on lithography defined surfaces and in solution" Materials research society, V **635**, p C6.2.1.

[Cherniavskaya 2003] Cherniavskaya O., Chen L., Weng V., Yuditsky L. and Brus L.. (2003). "Quantitative Noncontact Electrostatic Force Imaging of Nanocrystal Polarizability". J. Phys. Chem. V **107**, p 1525.

[Davis 2004] Davis J., Morgan A., Wrathmell L. and Zhao A., (2004). "Scanning probe technology in metalloproteins and biomolecular electronics", IEE Proc.Nanobiotechnol., V **151**, No. 2, p 37.

[Ding 2006] Ding K., (2006): "Architectures of DNA block copolymers", PhD dissertation, Johannes Gutenberg University., Germany.

en.wikipedia.org/wiki/Transmission_electron_microscope

en.wikipedia.org/wiki/X-ray_crystallography

[Erika 2003] Erika J., (2003) "Biotech boost for nanoelectronics, Proteins seen as a versatile platform for making tiny wires"**,** Technology Review.

[Fabio 2004] Fabio P., (2004). "A quantum mechanical study phosphotyrosyl peptide biding to the SH2 domain of p561ck tyrosine kinase with insights into the biochemistry of intracellular signal transduction events0", Biophys. Chem., V **109**, p 295.

[Hansma 2000] Hansma H.G., Pietrasanta L.I., Auerbach I.D., Golan R. and Holden P.A. (2000) "Probing biopolymers with the atomic force microscope: A review". J. Biomater. Sci. Polym, V **11**, p 675.

[Hartmann 1997] Hartmann U. (1997), "**An Elementary Introduction to Atomic Force Microscopy and Related Methods"**. University of Saarbrucken Publications. Saarbrucken, Germany.

[Israelachvili 1992] Israelachvili J. N., (1992). "Intermolecular and Surface Forces". 2nd edition; Academic Press: London.

[James 1999] James B. H. (1999). "MICA". The U.S. Bureau of Mines, V **51**, p 1.

[Jurveston 2004] Jurveston S. (2004): "Transcending Moore's Law with Moleculer Electronics and Nanotechnology". Nanotechnology Law and Business, March, 2004 Issue.

[Keller 1992] Keller D.J. and Chih-Chung C., (1992), "Imaging steep, high structures by scanning force microscopy with electron beam deposited tips", Surf. Sci., V **268**, p 333.

[Krauss 1999] Krauss T. and Brus L. (1999). "Charge, Polarizability, and Photoionization of Single Semiconductor Nanocrystals". Appl. Phys. Let. V **83**, No. p 23

[Lemke 1990] Lemke H., Göddenhenrich Th., Bochem H. P., Hartmann U., and Heiden C. (1990). "**Improved microtips for scanning probe microscopy**" Rev. Sci. Instrum. V 61, p 2538.

[Levy 2002] Levy I., Shani Z. and Shoseyov O. (2002). "Modification of polysaccharides and plant cell wall by endo-1,4-beta-glucanase and cellulose-binding domains", Biomol. Eng., V**19**, p 17.

[Lontie 1984] Lontie R., and Editor T., (1984). "Copper proteins and copper enzymes", CRC Press, Inc., Boca Raton, Fla., V **1**, p 241.

[Nirmal 1999] Krauss T.D. and Brus L. (1999), "Charge, Polarizability and Photoionization of Single Semiconductor Nanocrystals". Acc. Chem. Res. V **32**, p 407.

[NOVA Workforce Board 2003] NOVA Workforce Board (2003): **Nanotechnology: The Next Great Wave of Innovation, White Paper**, First edition.

[Polyakov 2003] Polyakov B., Erts D., Malinovskis U., Muiznieks I., Tuite E., (2003). "SPM studies of DNA architectures on Au(111) and mica surfaces", Institute of Chemical Physics, University of Latvia, Rainis blv, V **19**, LV-1586.

[Quintarelli 2006] Quintarelli E., Rosati L., Resmini A., (2006) "Facetag: Integrating Bottom-up and Top-down Classification in a Social Tagging System", presented at the EuroIA Conference 2006, Berlin (DE).

[Ross 2003] Ross R., Giuseppe M., Adriana B., Paolo V., Valentina A. and Roberto C., (2003). "A Protein-Based Three Terminal Electronic Device", Ann. N.Y. Acad. Sci., V **1006**, pp 187-197.

[Sarikaya 2003] Sarikaya, (2003). "Molecular biomemetics nanotechnology through biology". Nature Materials. V **2**. p 247.

[Staii 2001] Staii C.; Johnson A. T.; Pinto N. J., (2001) "Quantitative Analysis of Scanning Conductance Microscopy". Nano Lett., V 4, p 859.

[Tanaka 1999] Tanaka K., (1999). "Nanotechnology Towards the 21st Century", Thin Solid Film, V 341, p 120.

[Tapan 2001] Tapan K. S., Anjali P., Jana N.R., Wang Z.L. and Tarasankar P. (2001). "Size controlled synthesis of gold nanoparticles using photochemically prepared seed particles". Journal of Nanoparticle Research, V **3**, p 257.

[The White House-Office of the Press Secretary 2000] The White House-Office of the Press Secretary (2000): **National Nanotechnology Initiative: Leading to the Next Industrial Revolution**. January 2000.

[Wang 2003] Wang X., Dgany O., Dym O., Altman A., Shoseyov O. and Almog O., (2003). "Crystallization and preliminary X-ray crystallographic analysis of SP1, a novel chaperone-like protein Acta Crystallogr". D Biol Crystallogr. V **59**, p 512.

[Wang 2002] Wang X., Pelah D., Alergand T., Shoseyov O. and Altman A. (2002). "Characterization of SP1, a stress-responsive, boiling-soluble, homo-oligomeric protein from aspen". Plant Physiol, V **130**, p 865.

[Boncheva 2002] Boncheva M. and Whitesides G. M. (2002), "Beyond molecules: Self-assembly of mesoscopic and macroscopic components", Proc Nat Acad Sci. V **99**, p 4769.

www.biomers.net

www.nanotech-now.com/NanoWorld-release-08262004.htm

www.ntmdt.ru/SPM-Techniques/Principles/Spectroscopies/Force-distance_curves_mode20.html

www.keele.ac.uk/depts/ch/groups/csg/pat/pathome.htm

www.ntmdt-tips.com/catalog/golden/non/products/NSG10_50.html

www.ntmdt-tips.com/catalog/golden/cond/non/pt/products/NSG03_Pt_15.html

www.pacificnano.com/afm-modes_single.html

[Yao 2007] Yao H., Yi C., Tzang C.-H., Zhu J. and Yang M., (2007). "DNA-directed self-assembly of gold nanoparticles into binary and ternary nanostructures ", Nanotechnology, V **18**, p 015102.